Determining Active Oxidant Species Reacting with Organophosphate Pesticides in Chlorinated Drinking Water

Determining Active Oxidant Species Reacting with Organophosphate Pesticides in Chlorinated Drinking Water

By

Stephen E. Duirk, Daniel P. Cherney[†], Christopher J. Tarr[‡], and Timothy W. Collette
National Exposure Research Laboratory
Ecosystems Research Division
Athens, GA

[†]National Research Council

[‡]Student Services Authority

NOTICE

This work has been subject to external peer and administrative review, and has been approved

for publication as an EPA document. Mention of trade names or commercial products does not

constitute endorsement or recommendation for use.

ABSTRACT

Chlorpyrifos (CP) is an organophosphate (OP) pesticide that was used as a model compound to investigate the transformation of OP pesticides at low pH and in the presence of bromide and natural organic matter (NOM) under drinking water treatment conditions. Raman spectroscopy was used to determine which active chlorine species was responsible for the rapid oxidation of CP below neutral pH. Over the pH range of 2-11, three active chlorine species were identified with Raman bands of 725, 711, and 538 cm^{-1}. The first two bands were easily assigned to HOCl and OCl^- respectively. The 538 cm^{-1} band was identified as $Cl_2(aq)$ after bubbling chlorine gas through phosphate buffered water at pH 2. Either at low pH or in water treatment plants that use direct injection of $Cl_2(g)$, molecular chlorine rapidly reacts with CP transforming it to chlorpyrifos oxon (CPO). In the presence of bromide, the loss of CP was found to be accelerated when aqueous chlorine was added. It was found that bromide acts as a catalyst in the oxidation of CP to CPO via the formation of hypobromous acid (HOBr) at concentrations relevant to drinking water treatment. Also, NOM was found to not inhibit the oxidation of CP to CPO in the presence of free chlorine under the experimental conditions in this study. A previously developed screening-level model used to predict OP pesticide degradation pathways was modified to model the effects of both bromide and NOM. The model adequately described the oxidation of CP to CPO by free chlorine as well as the stability of CPO over the course of the experiment. This work demonstrated the applicability of screening-level models to predict the fate of OP pesticides under drinking water treatment conditions.

ACKNOWLEDGEMENT

TABLE OF CONTENTS

LIST OF TABLES

LIST OF FIGURES

EXECUTIVE SUMMARY

Environmental regulations require that all relevant routes of human exposure to anthropogenic chemicals be considered in risk assessments. Community water systems (CWSs) serve approximately 95% of the US population and potable water is considered a relevant route of exposure to anthropogenic chemicals. There is available monitoring data for important pesticides and toxic chemicals in drinking water sources (both surface and ground water). However, there is very little monitoring data for these chemicals or their degrades in finished drinking water. Limited experimental studies show that some chemicals are partially removed by physical water treatment processes (e.g., filtration, flocculation, etc.), and some are transformed by reactions that occur during chemical treatment (e.g., disinfection and softening). Transformation products of some contaminants have been shown to be more toxic than the parent compound.

This report is in partial fulfillment of the National Exposure Research Laboratory Task # 16608, "Fate of Pesticides and Toxic Chemicals During Drinking Water Treatment", under Goal 4, GPRA Objective 4.5, and GPRA Sub-objective 4.5.2. The goals of this research task are to: 1) provide chemical-specific information on the effects of water treatment for high-priority pollutants, 2) provide physicochemical parameters for transformation products, and 3) develop predictive models for forecasting treatment effects that cross chemical class and treatment conditions.

Drinking water sources are a complex matrix of inorganic anions and cations and natural organic matter (NOM). Because of this complexity, it is exceedingly difficult to predicting the potential transformation of anthropogenic compounds under conditions that simulate drinking water treatment. Therefore, it is necessary to identify specific components in drinking water matrices that could significantly influence the transformation of anthropogenic chemicals (e.g.,

organophosphate (OP) pesticides). Also, the effect of these native aqueous constituents could be dependent on other drinking water plant operational parameters such as pH adjustment or application of disinfectants.

Results of experiments reported here demonstrate that the change in risk associated with the transformation of OP pesticides due to drinking water chlorination practices is a very complex issue. For example, pH of the finished water can significantly affect the rate of OP pesticide transformation. Previous work has shown that oxidation of OP pesticides by free chlorine near neutral pH leads very rapidly to a more toxic transformation product (i.e., oxons). Also, OP pesticides are susceptible to chlorine-assisted hydrolysis above neutral pH, which leads to a less-toxic transformation product. Below pH of 6, the oxidation of OPs can proceed much more rapidly than expected. This phenomenon has been observed by others in the drinking water community examining the loss of other anthropogenic compounds in the presence of free chlorine. Therefore, we chose to investigate this phenomenon in order to determine its relevance to drinking water treatment. Additionally, two native aquatic constituents (i.e., bromide and NOM) were investigated to determine their effect on the transformation of OP pesticides. It was hypothesized that bromide could accelerate the rate of OP transformation, while the presence of NOM was expected to decrease the rate of OP transformation due to the fact that NOM could act as a sink for active oxidants commonly used in drinking water treatment.

Raman spectroscopy was used to determine the presence of active chlorine species over the pH range of 1-11. Over the pH range 5-11, unique Raman bands were identified and associated with hypochlorous acid (HOCl) and hypochlorite ion (OCl$^-$) with Raman shifts of 725 and 711 cm^{-1} respectively. As the pH was lowered below pH 5, in-growth of a band at 538 cm^{-1} appeared while the band at 725 cm^{-1} disappeared. This low-pH active chlorine species was

identified as Cl_2(aq). Molecular chlorine in the aqueous phase is a more potent oxidant than HOCl. The relevance of this to the drinking water industry is that many plants use chlorine gas to chlorinate potable water. Cl_2(g) does hydrolyze to HOCl and OCl⁻ quickly near neutral pH; however, its selective and rapid reactivity with not only OP pesticides but other anthropogenic chemicals is a factor in determining the risk associated with drinking potable water contaminated with anthropogenic chemicals.

Bromide and NOM were investigated to determine their effect on the transformation rate of OP pesticides. Bromide was found to significantly increase the rate of chlorpyrifos (CP) transformation. This is due to the oxidation of Br⁻ by HOCl resulting in the formation of hypobromous acid (HOBr), which is a more potent oxidant than HOCl. Since the formation of HOBr is pH dependent, a screening-level model that forecasts the concentrations of all reaction products as a function of pH, chlorine dose, OP pesticide concentration, bromide concentration, and time after chlorine dosing was developed. Using this simple model, the concentrations of CP, chlorpyrifos oxon (CPO), and 3,5,6-trichloro-2-pyridinol (TCP) can be adequately described under a variety of scenarios that are similar to drinking water treatment conditions using an apparent rate coefficient describing the reaction between HOBr and CP. In the presence of NOM, the model was found to predict the transformation of CP to CPO as well as the degradation of CPO to TCP in the presence of free chlorine.

The work reported here demonstrates the "proof-of-concept" towards the development of a comprehensive modeling tool for OP fate in drinking water treatment plants and distribution systems. Following the reported work, we have now begun to apply the experiments and models to other OP pesticides that were judiciously selected to reflect the full range of chemical structure variability in this class. Our objective is to develop predictive models that associate

relative rates of reactivity to structural variability. This will allow decision makers to rank and prioritize chemicals found in drinking water sources according to potential risk. Also, we are currently in the process of investigating chloramination disinfection practices on the transformation of OP pesticides.

1   INTRODUCTION

The Food Quality Protection Act of 1996 (FQPA) requires that all pesticide chemical residuals in or on food be considered for anticipated human exposure. Drinking water is considered a potential pathway for dietary exposure, but there is reliable monitoring data for only the source water. For example, the United States Geological Survey (USGS) completed a national reconnaissance survey known as NAWQA (National Water Quality Assessment) to help define human exposure to various contaminants (1). For the NAWQA survey, 90 pesticides (and some selected metabolites) were chosen as target chemicals to monitor in US drinking water sources. However, there is a relative dearth of information on occurrence of pesticide residuals and pesticide metabolites in finished drinking water. Two surveys have been conducted for a few community water systems examining pesticide concentrations in the source and finished drinking water (2,3). Neither of these studies thoroughly examined the effect of each treatment process on a single slug of water, hence only the influent and effluent of each treatment facility could be qualitatively discussed with respect to overall removal efficacy. Also, these studies did not account for the treatment plant hydraulic retention time, thus it was not possible to ensure that influent and effluent samples were properly paired. Clearly, more thorough occurrence studies that include monitoring drinking water for both pesticides and their expected transformation products are needed.

Chlorination is the most commonly used chemical disinfection process for community water systems (4) and is known to react with numerous pesticides. For example, four s-triazines were found to degrade in the presence of free chlorine ($HOCl + OCl^-$) (5,6). Atrazine was also found to be significantly degraded by ozone (7); however, subsequent chlorination of the ozonated effluent had very little affect on the concentration of residual atrazine or its ozone degradation products (2). Also, some carbamate pesticides have been shown to react with free

chlorine while other members of this pesticide class were found to be stable in chlorinated water. For example, carbaryl and propoxur do not react with free chlorine; but aldicarb, methomyl, and thiobencarb do exhibit significant reactivity (8-10). These findings demonstrate that free chlorine reactivity with different members in a specific class of pesticides can vary significantly due to chemical structure variations. Therefore, it is prudent to study the fate and transformation pathways of entire chemical classes, using class members that exhibit systematic structural variations and employing carefully selected experimentation and numerical modeling.

When chlorine reacts with the phosphorothioate subgroup of organophosphate (OP) pesticides, the thiophosphate functionality (P=S) can be oxidized to its corresponding oxon (P=O) (11-13). The resulting oxons are typically more potent than the parent as an inhibitor of acetlycholinesterase, an enzyme necessary for proper function of the nervous system (13). Duirk and Collette, (14) elucidated the fate of chlorpyrifos (CP) and its transformation products over the pH range of 6-11. They were able to model the loss of CP and chlorpyrifos oxon (CPO) to the stable end-product of 3,5,6-trichloro-2-pyridinol (TCP) over this pH range in buffered deionized water systems. However, other factors such as pH below 6, bromide ion, and natural organic matter can significantly influence the transformation rate of CP.

Several recent papers in drinking water literature have reported free chlorine oxidation phenomena that stray from expected results as the pH was lowered in the course of kinetic experiments with various anthropogenic chemicals (15-17). Specifically, a dramatic increase in reaction rate was observed in solutions when the pH was lowered below approximately 5. The same trend has been observed while studying the free chlorine oxidation of CP, and a kinetic plot depicting this phenomenon is displayed in Figure 1. Initially, the observed reaction rate was assumed to be relatively constant as the pH was lowered below the point where HOCl was the

principal species and the OCl⁻ concentration was insignificant. This result was expected because HOCl is generally assumed to be the predominate oxidant in free chlorine solutions. However, since the observed rate coefficient increased dramatically as pH was dropped below 5, it was clear that there was another chlorine species in solution, more potent as an oxidant than HOCl.

At least two competing hypotheses have been put forward by various researchers regarding the identity of the species responsible for this rapid oxidation. Specifically, some researchers have proposed H_2OCl^+ as the oxidant (18), and other researchers have proposed $Cl_2(aq)$ (17). In literature, there are no thorough studies designed to rigorously determine the identity and speciation profile of this potent oxidant. It appears that the H_2OCl^+ species was first proposed as an active species at low pH in 1962 by Arotsky and Symons (19) in their discussion of halogen cations. Although they did not measure the pK_a for H_2OCl^+, it was estimated to be between -3 and - 4 (19). Some publications have discussed the existence of the H_2OCl^+ cation (20,21) as part of a reverse hydrolysis reaction. Despite the low proposed pK_a, many chlorination (15,16,18,22,23) and other oxidation (24) studies have either proposed or discussed H_2OCl^+ as the reactive, oxidative species in low pH aqueous solutions. There have been a few publications disagreeing with the hypotheses involving this species, but these are much fewer in number and are found in the inorganic chemistry literature (25,26).

The presence of bromide ion (Br⁻) in drinking water sources has been of interest to the drinking water industry for several reasons. Bromide ion can be oxidized by ozone (O_3) resulting in the formation of bromate ion (BrO_3^-) (27). Bromate is a suspected carcinogen and is regulated under Stage 1 of the Disinfection/Disinfection Byproducts (D/DBP) Rule at a maximum contaminant level (MCL) of 0.01 mg/L. Bromide can also be easily oxidized to hypobromous acid in the presence of free chlorine (28), it is a stronger oxidant that HOCl,

$$HOCl + Br^- \longrightarrow HOBr + Cl^- \qquad k_{HOCl,Br} = 5.6 \times 10^6 \ M^{-1}h^{-1} \qquad (1)$$

$$HOBr + H_2O \rightleftharpoons OBr^- + H_3O^+ \qquad pK_a = 8.8 \qquad (2)$$

and the pK_a of hypobromous acid is 8.8 (28). In the presence of excess chlorine, all bromide present will be oxidized to active bromine (29). Over the pH range of 6.5-9, which is the pH range of the National Secondary Drinking Water Standards, most of the active bromine present will be in the HOBr form (i.e., the active oxidant). Therefore, it is believed that the presence of bromide under drinking water treatment conditions could accelerate the transformation of anthropogenic chemicals. For example, the rate coefficient for HOBr reacting with pyrene was found to be 2 orders of magnitude faster than HOCl in aqueous solutions (30). In the presence of natural organic matter (NOM), both brominated and chlorinated oxidants react with NOM resulting in the formation of disinfection byproducts (DBPs) (31,32). The brominated DBPs are believed to be more carcinogenic than their chlorinated analogs (33). Westerhoff et al., (34) conducted a nationwide survey of 101 drinking water sources and found that the average bromide concentration was ≈ 1.25 μM. Since bromide is a relatively ubiquitous and 90% of community drinking water systems use chlorine for both primary and secondary disinfection, the presence of bromide ion in drinking water sources could affect the rate of organophosphorus (OP) pesticide transformation in chlorinated drinking water.

The presence of NOM in drinking water sources has also been a primary concern for the drinking water industry. The physical-chemical properties of NOM are a function of decaying organic matter from both terrestrial and aquatic sources, environmental conditions, and microorganisms present in the watershed (35). Hence, the composition and concentration of NOM in source waters fluctuates from source to source and often varies within each source depending on conditions such as rainfall, change in seasons, and temperature. When chlorine

reacts with NOM, it often results in the formation of DBPs (33). The electron density (i.e., aromaticity) of NOM is often expressed as specific ultraviolet absorbance (SUVA), which is the ratio of ultraviolet absorbance of the NOM at a specific wavelength divided by the total organic carbon concentration (TOC) in mg-C/L. This specific physical-chemical property of NOM has been found to correlate to reactivity of NOM with free chlorine and serve as a reliable surrogate for DBP formation (36,37). Since both chlorinated and brominated oxidants react with NOM (38), the presence of NOM can potentially act as a sink for active oxidants in potable water. Thus, its presence can impact the rate of OP pesticide transformation under drinking water treatment conditions.

One purpose of this study was to identify active oxidants under drinking water treatment conditions. Toward this end, Raman spectroscopy was used to determine active chlorine species present over the pH range of 1-11 in a solution where active chlorine to chloride ion molar ratios were equivalent (equal-molar chlorine solution: ECS). Also, a low chloride ion active chlorine solution (low-chloride chlorine solution: LCS) was prepared to assist in the identification of active chlorine species as a function of pH. Kinetic studies with CP in the presence of both ECS and LCS were conducted to investigate CP transformation below pH 6. Bromide ion was investigated to determine the effect it has on transformation of CP in the pH range of 7-9. Also, the influence of NOM on the transformation of CP was investigated over the pH range of 7-9.

The work reported here serves to further elucidate the OP transformation pathways under drinking water treatment conditions. The long-term objective is the development of a comprehensive modeling tool for OP fate in drinking water treatment plants and distribution systems. This will allow decision makers to rank and prioritize chemicals found in drinking water sources according to potential risk. The goal of these experiments was to incorporate these

important matrix effects into our models so that the models can be applied to actual drinking

water treatment scenarios.

2　　EXPERIMENTAL PROCEDURES

2.1　Materials

Chlorpyrifos (99.5%), chlorpyrifos oxon (98.7%), and 3,5,6-trichloro-2-pyridinol (99%) were purchased from ChemService (West Chester, PA). Commercial 10-13% sodium hypochlorite (NaOCl), purchased from Aldrich (Milwaukee, WI), contained equal-molar amounts of OCl^- and Cl^-. Aqueous stock solutions and experiments utilized laboratory prepared deionized water (18 MΩ cm^{-1}) from a Barnstead ROPure Infinity™/NANOPure ™ system (Barnstead-Thermolyne Corp., Dubuque, IA). Chlorine gas (99.9% purity) was purchased from Matheson Tri-Gas (Montgomeryville, PA). Filters with pore size of 0.45 μm were purchased from Millipore (Billerica, MA). Phosphate and carbonate salts used for buffer solutions were dissolved in deionized water and filtered through a 0.45 μm filter, which was pre-rinsed with deionized water. The pH for the experiments was adjusted with either 1 N H_2SO_4 or NaOH unless otherwise noted. All other organic and inorganic chemicals were certified ACS reagent grade and used without further purification. The glassware and polytetrafluoroethylene (PTFE) septa used in this study were soaked in a concentrated free chlorine solution for 24 hours, rinsed with deionized water, and dried at 105 ^{o}C prior to use. All chlorination experiments were conducted at constant temperature (25±1°C).

Water was collected form the Athens-Clarke County (ACC) water treatment plant and used in some experiments. The ACC water treatment facility uses conventional physical-chemical surface water treatment (i.e., coagulation, flocculation, sedimentation, and dual media filtration) prior to chlorination. Water was collected prior to chlorination and the NOM and source water characteristics are shown in Table 1. The $SUVA_{254}$ of the ACC effluent was 1.61 L/mg-m, which indicates a low aquatic humic substance concentration in this water (36).

7

2.2   *Methods*

2.2.1   *Spectroscopic Studies of Active Chlorine Species*

For speciation studies, Raman spectra were collected of free-chlorine solutions as a function of pH (at least 20 points) over the range of approximately 1 to 12. The commercial sodium hypochlorite solution (ECS) was diluted with deionized water to a stock solution with a free chlorine concentration of 262.0 mM to more closely match that of the low chloride solution (LCS) that was prepared in our lab. Total free chlorine concentration was again determined via Standard Method 4500-Cl F DPD-FAS titrimetric method (39). The final concentrations of free chlorine in the ECS solutions monitored with Raman spectroscopy were 26.2, 13.1 and 6.6 mM. The pH of 50 mM phosphate buffer was raised with 5 N sodium hydroxide and lowered with a 2 N sulfuric acid solution. The cuvette used for Raman work was relieved of chlorine demand by soaking it in a concentrated free-chlorine solution overnight and rinsing it several times with deionized water. Samples for Raman analysis were prepared by adding an appropriate amount of buffer directly to the cuvette, followed by the addition of free-chlorine solution. The cuvette was then rapidly capped, and inverted several times for mixing. Minimal headspace was left in the capped cuvette to minimize the possible loss of a volatile species in a low pH solution. (There was ~ 100 μL of gas volume between the solution and the cap.) The filled cuvette was then placed into a sample holder and the Raman spectra were acquired. Unless otherwise noted, the time for each acquisition was 5 s. To improve the signal-to-noise ratio in the spectrum, 200 of these 5 s acquisitions were co-added (i.e., averaged). After acquisition of the Raman spectra, the samples were transferred into a vial that had been relieved of chlorine demand and the final solution pH was recorded.

Some of our experiments were carried out with a free-chlorine solution containing a low concentration of chloride ion, LCS. Our method for preparing this solution, which was adapted

from Reinhard and Stumm (40), involves complexing and removing excess chloride ion from hypochlorous acid/hypochlorite preparations. First, all glassware was soaked in a concentrated free-chlorine solution to satisfy any chlorine demand. The glassware was rinsed with deionized water and dried at 105 °C prior to use. To a 250 mL graduated cylinder, sodium hydroxide (2.5mL of a 1 N solution) was added to deionized water for a final volume of 250 mL. Mercuric oxide (8.33g) was added to the graduated cylinder and the solution was stirred for 10 min. Chlorine gas was then bubbled through the HgO/NaOH/water solution for 3 min and this solution was stirred for 1 h. After the stirring time had elapsed, the solution was filtered through a 0.45 μm filter that had been pre-rinsed with 1.5 L of deionized water. The filtrate was then distilled at 90°C into sodium hydroxide (2.5 mL of a 0.1 N solution). The distillate was stored at 4°C until further used.

The amount of chloride ion in the LCS was determined in a multi-step process. First, using the Standard Method 4500-Cl F DPD-FAS titrimetric procedure (39), we determined that the total free-chlorine concentration was 202.5 mM. (At the alkaline pH of this solution, the total free-chlorine concentration is essentially equal to the OCl^- concentration.) Next, an aliquot of the LCS was reduced with excess sodium sulfite, thereby converting all species of chlorine to chloride ion. Then, using ion chromatograph with chemical suppression, we determined that the chloride ion concentration in the reduced aliquot was 220.0 mM. Therefore, by difference, we determined that the chloride ion concentration in the LCS was 17.5 mM. This method of producing a low chloride ion solution was effective – the free chlorine to chloride ion molar ratio in our prepared LCS was 11.6:1, whereas in the commercial ECS the ratio was 1:1.

Many studies have been published on the absorption of chlorine into water (41) and on the kinetics of HOCl production at various temperatures (42-44) and ionic strengths (44). This

reaction has been shown to proceed more rapidly at both higher temperature and higher ionic strength, (42-47) and experimental evidence has been obtained with several buffers arguing that the reaction involves base-assisted hydrolysis (48-50). A low pH free-chlorine solution was prepared by bubbling chlorine gas through a solution of 50 mM phosphate buffer for approximately 20 sec. The initial pH of the solution was 1.8 and the final pH was 1.4 and the color of the solution changed from clear to yellow. We report experiments here using this solution, which was assigned the acronym BCS to denote Bubbled Chlorine Solution

2.2.2   *Chlorpyrifos Kinetic Experiments with Bromide and NOM*

For all CP oxidation experiments, CP was spiked by adding 0.5 mL of a 4 mM stock solution in ethyl acetate into an empty 4 L borosilicate glass Erlenmeyer flask. A gentle flow of nitrogen gas was used to evaporate the ethyl acetate and then 4 L of deionized or ACC water was added to the flask. The solution was slowly stirred and allowed to dissolve for 12 hours resulting in an aqueous concentration of 0.5 μM. Experiments studying the effect of bromide, bromide was added to the aqueous system prior to chlorination. CP chlorination kinetic experiments were conducted under pseudo-first-order conditions: total chlorine to chlorpyrifos molar ratios of 20:1, 50:1, and 100:1 were used. Chlorine was added to solutions under rapid mix conditions achieved with a magnetic stir plate and a PTFE coated stir bar. All kinetic experiments used to estimate rate coefficients measured at least 87% loss of parent compound.

Above pH 8, 10 mM carbonate $[CO_3]_T$ buffer was used to maintain pH. The purchased free chlorine solution was first diluted to 250 mM then added to the aqueous system containing 0.5 μM chlorpyrifos and carbonate buffer in a 2 L Erlenmeyer flask. Fourteen aliquots from the large 2 L reactor were then placed into 128 mL amber reaction vessels with PTFE septa and stored in the dark. In the pH range of 6.0-7.5, the rate of CP loss in the presence of free chlorine

was very fast. Therefore, fourteen 100 mL aliquots of the 2 L aqueous system containing 10 mM phosphate buffer, $[PO_4]_T$, and 0.5 μM CP were placed in 250 mL amber Erlenmeyer flasks. Then each flask was individually dosed with the appropriate amount of chlorine.

At each discrete sampling interval, two reaction vessels were sacrificed in their entirety. One vessel was used to determine total free chlorine concentration ($[HOCl]_T = [HOCl] + [OCl^-]$) via Standard Method 4500-Cl F DPD-FAS titrimetric method (39). In the other vessel, free chlorine residuals were quenched and the pH of a 100 mL sample was then adjusted to 2 for analysis of CP and its degradation products.

Chlorine residuals were quenched with sodium sulfite in 20% excess of the initial free chlorine concentration. Both sodium sulfite and ascorbic acid were tested as quenching agents to determine if they affected the stability or recovery of CP, CPO, or TCP. Control studies compared the recoveries of all three analytes in water without chlorine present after two hours at room temperature with and without a quenching agent present. Sodium sulfite had no apparent effect on the recovery of any of the three analytes. However, ascorbic acid reduced the recovery of CP by about 5.1% and increased the recovery of CPO by about 7.6%, as compared to both the sodium sulfite quenched samples and the samples with no quenching agent present. Furthermore, ascorbic acid has previously been found to react with organophosphate pesticides (51). Therefore, ascorbic acid was not used to quench chlorine residuals in this work.

2.3   *Instrumentation*

The Raman spectra were acquired with a Kaiser Optical Systems (Ann Arbor, MI) HoloProbe, using 532 nm laser excitation from a Coherent™ (Santa Clara, CA) Verdi V Series frequency-doubled YVO_4 laser. This type of Raman instrument has been fully described elsewhere (52,53). Briefly, laser light was coupled to a remote probe head via a 1.9 m long fiber-optic cable. Raman scattering and luminescence were removed from the excitation optical

11

train via a holographic grating and spatial filter within the probe head. This filtered laser light

was brought to a focus with a 10x microscope objective (Olympus) approximately in the center

of a standard quartz cuvette with a screw cap. The power of the laser light at the cuvette was

approximately 220 mW. Raman scattered photons from the solution were collected by the

microscope objective along the same path as the excitation laser beam (i.e. 180° backscattering

geometry), and were coupled to a separate 1.9 m fiber-optic cable for delivery to the f/1.8 axial

transmissive-type spectrograph. The probe head contained a holographic notch filter placed

along the collection path such that only inelastically scattered light was inputted into the fiber.

Inside the spectrograph the scattered light was passed through another holographic notch filter to

further remove elastically scattered light returning from the probe head. The Raman scattered

light was then focused through a 50 μm slit and directed through a holographic grating with

double transmission layers. These layers permit two regions of the dispersed Raman spectrum to

be stacked and simultaneously focused onto the back-illuminated CCD detector (Andor

Technology model DU420). This configuration permitted the acquisition of the entire Raman

spectrum with a useable Stokes Raman shift of about 4450 to 100 cm^{-1} in a single exposure with

about 5 cm^{-1} spectral resolution. The CCD detector was thermoelectrically cooled to -65°C and

contained 1024x 256 pixels.

A Kaiser Optical Systems, Inc. HoloLab calibration accessory was used to correct both

the frequency and intensity of the Raman spectra. Briefly, each spectrum was frequency-

corrected based on previously measured lines from a neon bulb. Also, each spectrum was

intensity-corrected based on a previously measured NIST-traceable, broadband light source (i.e.,

a tungsten bulb) that was powered by a current regulated power source for consistent spectral

output.

Analysis of a Raman spectrum required the subtraction of a 50 mM phosphate buffer spectra that was the same pH of the chlorine-containing solutions. The pH of the buffer was no more than a few hundredths of a pH unit different from that of the associated solution. The bands in the spectrum were then analyzed by fitting a Gaussian-Lorentzian mixed curve in GRAMS/32 (Thermo Galactic). Since the HOCl and OCl⁻ bands overlapped with each other, the center frequency and band width for these two species were determined with spectra that were not near the pKa of hypochlorous acid. These two parameters were then held constant throughout the analysis and the band areas were determined for each spectral acquisition. In addition, the band associated with atmospheric nitrogen was averaged and used, as has been previously described (54) to correct the band areas corresponding to the chlorine species for any changes in instrumental conditions (e.g., alignment, laser power fluctuations, etc.).

We sought to use these individual Raman band areas to construct chemical speciation plots. For our purpose, a speciation plot is useful when it depicts the fractions of the total analytical concentration that belong to the various species in solution as a function of pH. Unfortunately, individual band areas could not be used directly to construct such plots because we could not assume that Raman scattering cross sections of the various species were equal. However, at the highest analytical concentration of free chlorine in ECS solutions examined by Raman spectroscopy (26.2 mM), it was possible by varying pH to obtain three individual Raman spectra, each of which uniquely contained appreciable intensity for only one of the three observed species. From these three spectra, we estimated an apparent Raman scattering cross section for each of the three species. Then, using these apparent cross sections, we calculated the intensity that we would observe for a given species at a given analytical concentration if 100% of the analytical concentration existed in that form. Individual Raman band area collected at the

various pH's for a given analytical concentration were then divided by this quantity in order to "normalize" them. These normalized band intensities, which ranged from nominal values of 0 to 1 were used in speciation plots to approximate the fractions of the total analytical concentration that belonged to the various species in solution as a function of pH.

CP and its degradation products were extracted from water using C-18 solid phase extraction cartridges purchased from Supleco (Bellefonte, PA). The 100 mL sample was pre-adjusted to pH $\leq$ 2 to increase the recovery of TCP ($pK_a = 4.55$) on the solid phase adsorbent (55). Then, the sample was spiked with 1 μM of phenthorate (internal standard), mixed thoroughly by hand for two minutes, passed through the SPE cartridge at an approximate flow-rate of 7 mL/min, and eluted with 3 mL of ethyl acetate. Quantification for each analyte was compared to eight extracted standards over the concentration range of 0.01 to 1 μM. A Hewlett-Packard 6890 GC equipped with a 5973 MSD was used to analyze CP, CPO, and TCP. GC conditions were as follows: 30-m Restek Rtx-200 column with a 0.25-mm ID and 0.5-μm film thickness. The temperature profile was: 100 °C for 5 minutes, 100 to 250 °C at 10 °C/minute, and then held at 250 °C for 25 minutes. Mass balances of 80% or greater were obtained for each experiment.

UV-Vis spectra were acquired with a Shimadzu 1700 UV-Vis spectrometer (Shimadzu Scientific, Columbia, MD). Total organic carbon (TOC) was measured using a Shimadzu TOC 5000 (Shimadzu Scientific, Columbia, MD) and calibrated according to Standard Methods 505A (39). Ion chromatography was performed on a Metrohm (Houston, TX) MIC-2 ion chromatograph with chemical suppression. All pH measurements were obtained with an Orion 940 pH meter using a Ross combination electrode from Fisher Scientific (Pittsburgh, PA).

3   RESULTS AND DISCUSSION

3.1   *Spectroscopic Studies of Active Chlorine Species*

As discussed earlier, there was a large increase in the rate of aqueous free chlorine

oxidation for chlorpyrifos when the pH was decreased below ~ 5. This behavior, which is

similar to that recently reported with other anthropogenic chemicals (15,17,56,57), suggests the

presence of an oxidant other than OCl^- and HOCl, and more potent than either, that is formed as

the pH decreases below 5. To firmly establish the existence of this third species, and to

determine whether it is Cl_2 (aq) or H_2OCl^+, Raman spectra of the aqueous free chlorine ECS

solution (26.2 mM) were collected over a pH range from approximately 1 to 12. Across this pH

range, three Raman bands appeared in the spectra due to various chlorine species in solution.

Specifically, a band at 711 cm^{-1} was observed to increase in intensity as the pH was increased

above 6, and its intensity was relatively constant above pH of ~ 9.5. A second band at 725 cm^{-1}

was observed to increase in intensity as the pH was lowered from 9 to 6, and its intensity

decreased as the pH was lowered below ~ 5. Finally, a third band at 538 cm^{-1} was observed to

increase in intensity as the pH was lowered below 5. The normalized areas of these bands are

plotted over the entire pH range in Figure 2A.

Figure 2B shows spectra of chlorine acid species in solution at four discrete pHs (11.96,

7.46, 4.59, and 2.73) with the aqueous phosphate buffer subtracted. Bands in the figure are

labeled according to the species to which they are attributed. The band at 711 cm^{-1} is confidently

attributed uniquely to the OCl^- species and the band at 725 cm^{-1} uniquely to the HOCl species, in

agreement with an earlier study (58). The in-growth of a Raman band at 538 cm^{-1} as the pH is

lowered below 5 supports the presence of a third chlorine species. We believe this band at 538

cm^{-1} can be attributed uniquely to the species that is responsible for the unexpectedly rapid

oxidation of anthropogenic chemicals that is observed in free chlorine solutions as pH decreases below 5.

Raman spectroscopy has been demonstrated as an effective method for determining the equilibrium constants of organic species in aqueous solution (54). By monitoring monotonic changes in spectra, the amount of each species can be quantified at each pH studied. This general method is applied to the current experiment to model chlorine species in aqueous solution. The pK_a for the protonation of OCl^-, described by:

$$HOCl \rightleftharpoons OCl^- + H_3O^+ \tag{3}$$

can be readily approximated by monitoring the Raman-active vibrational bands of the species HOCl and OCl^- (at 725 and 711 cm^{-1}, respectively) as a function of pH. Specifically, for a simple isolated protonation event of this type, the pK_a can be approximated as the pH at which the normalized intensities of the HOCl and OCl^- bands are equal because, according to the Henderson-Hasslebach equation, when [HOCl] = [OCl^-], the

$$pH = -log\ K_1 = pK_1 \tag{4}$$

and

$$K_1 = [OCl\text{-}]\ [H_3O^+]/[HOCl] \tag{5}$$

(Although it would be accurate in this case to label the equilibrium constant as K_a, for this work the more generic K_1 and K_2 to denote constants for the equilibria discussed at high and low pH, respectively. For simplicity, concentration-based equilibrium constants will be presented. Using the extended Debye-Hückel equation (59) the calculated activity coefficients for all charged species discussed herein and have determined that, at the concentrations used in this work , activity-based equilibrium constants do not differ significantly from those based on concentration. Specifically, for determination of pKs, the differences were calculated to be

between 0.7 and 1.2% for the high pH event and 1.3 to 6.4% for the low pH event for all

equilibrium cases and concentrations considered. For these calculations, activity coefficients of

all neutral species were assumed to be 1.

Furthermore, the species arising at a lower pH can be described by either equation 6 or 7,

as discussed in the Introduction:

$$H_2OCl^+ \rightleftharpoons H_3O^+ + HOCl \tag{6}$$

$$H_2O + Cl_2 \rightleftharpoons H_3O^+ + HOCl + Cl^- \tag{7}$$

If equation 6 is correct, then the low-pH species is formed from a simple protonation event like

that described in equation 3. On the other hand, if equation 7 is correct, the equilibrium is more

complicated, involving species other than a proton and a protonated/deprotonated pair.

A convenient way to distinguish between the two situations described by equations 6 and

7 was to monitor the relative concentrations of HOCl and the low-pH form as a function of pH as

the absolute concentration of total chlorine was varied. This was achieved by preparing

speciation plots such as that shown in Figure 2A for several chlorine concentrations. If equation

6 was the proper description, the pH at which the normalized intensities of the bands for the low-

pH form and HOCl are equal would approximate the pK_a and this observed pK_a would not vary

as a function of total free chlorine. Specifically, for equation 6 (as with equation 3), when

$[HOCl] = [H_2OCl^+]$, the

$$pH = -log\ K_2^{H2OCl+} = p\,K_2^{H2OCl+} \tag{8}$$

where

$$K_2^{H2OCl+} = [HOCl]\ [H_3O^+]\ /\ [H_2OCl^+] \tag{9}$$

Alternately, if equation 7 was the proper description, the pH at which the normalized intensity of the bands were equal would change as a function of total free chlorine. Specifically, for equation 7, when [HOCl] = [Cl$_2$], the

$$pH = -log \ K_2^{Cl2} + log \ [Cl^-] = p \ K_2^{Cl2} + log \ [Cl^-] \quad (10)$$

where

$$K_2^{Cl2} = [HOCl] \ [Cl^-] \ [H_3O^+] \ / \ [Cl_2] \quad (11)$$

The commercial reagents used to prepare free-chlorine solutions (ECS) were equimolar in HOCl and Cl$^-$. So, as the free chlorine concentration is increased, [Cl$^-$] will increase. Thus, from equation 10, we would expect the pH at which the normalized intensity of the bands are equal to increase as the free chlorine concentration increases in ECS solutions if equation 7 is the proper description of the low pH behavior.

Full speciation plots, using normalized Raman band intensities, for three different commercial total free chlorine solutions (ECS solutions) are displayed in Figure 3. In order to determine if the apparent pK for either equilibrium changed as a function of chlorine concentration, the normalized band intensities were fit using standard equations that describe the concentration profiles of polyprotic acids (60). To present these equations, we assigned K$_2$ as the equilibrium constant for the low pH event described by equation 9 or 11 and K$_1$ for the higher pH event described by equation 5. For these generalized equations, the amount of each component (α_i) is described in terms of the total amount of the acid or base present. In this case: (60)

$$\alpha_0 = \frac{[lowpHform]}{C_T} \quad (12)$$

$$\alpha_1 = \frac{[HOCl]}{C_T} \tag{13}$$

$$\alpha_2 = \frac{[OCl^-]}{C_T} \tag{13}$$

where C_T = [low pH form] + [HOCl] + [OCl$^-$]. It is important to note that the sum of the α_i components must be equal to 1 under every condition. The numerical value of each α_i component was obtained by utilizing the following equations: (60)

$$\alpha_0 = \frac{[H_3O^+]^2}{[H_3O^+]^2 + K_2[H_3O^+] + K_2K_1} \tag{14}$$

$$\alpha_1 = \frac{K_2[H_3O^+]}{[H_3O^+]^2 + K_2[H_3O^+] + K_2K_1} \tag{15}$$

$$\alpha_2 = \frac{K_2K_1}{[H_3O^+]^2 + K_2[H_3O^+] + K_2K_1} \tag{16}$$

The model was fit to the data by using a least-squares analysis and allowing the values for K_2 and K_1 to vary in order to minimize the sum of the squared residuals. The fit of the model in the top graph of Figure 3 most closely matches the experimental data because it was used to determine the apparent Raman scattering cross-section for each species. Subsequent plots of experimental data for 13.1 mM and 6.6 mM solutions deviate slightly from the model because the spectral correction with the nitrogen band (as described in the Experimental section) cannot perfectly encompass all variations in the instrument over long periods of time. (Note that all of the data in Figure 3 was collected over a time period of 60 days). Furthermore, the greatest variation between experimental data and the model is seen in the amounts of HOCl and OCl$^-$.

This is likely due to these bands not being completely resolved from one another, limiting the accuracy of the curve fitting routine.

The vertical line on the right in Figure 3 indicates the apparent pK_a (i.e. pK_1) for the protonation of OCl⁻ that occurs between pH 7 and 8 for each concentration of free chlorine. This line indicates that the pKa of hypochlorous acid is approximately 7.50, which agrees very well with the previously published result of a pKa near 7.5 (44). Indeed, the pK_a for each concentration was identical to the significant digits that we can accurately report. On the other hand, it is evident, as shown by the line on the left in Figure 3, that the apparent pK for the low pH equilibrium does not occur at the same pH regardless of concentration. The apparent pK increases from 1.25 to 2.11 as the concentration of free chlorine in solution is increased. The inconsistent location of the pK in this equilibrium strongly suggests that a protonation event is not the source of the change and that equation 7 is the proper description of the low-pH behavior. Indeed, the direction of the change – an increase in apparent pK as the free chlorine concentration is increased – was predicted (in equation 8) when equation 7 was the proper description. Furthermore, the magnitude of the change in apparent pK on going from 6.6mM to 26.2 mM – over 65% – was much larger than could be explained by changes in activity coefficients over this concentration range. Indeed, changes in activity coefficients alone would result in a change in apparent pK over this concentration range of less than 5%.

To further investigate the hypothesis that Cl_2 was the correct assignment for the low-pH form of aqueous free chlorine, a Raman spectrum was acquired of a solution (BCS) that had been prepared by bubbling chlorine gas through an acidic 50mM phosphate buffered solution for approximately 20 s. The pH of the BCS solution was intentionally kept low during preparation for comparison to the diluted, acidic ECS solutions that were monitored earlier. The Raman

20

spectrum of the acidic BCS solution is shown as trace A in Figure 4. The band at 538 cm^{-1}, as previously observed in low-pH ECS solutions prepared from HOCl, was very prominent in the BCS spectrum and is much larger than the observed HOCl vibration (at 725 cm^{-1}). The Raman spectrum of a diluted ECS solution at approximately the same pH is also shown, as trace B, in Figure 4. Our hypothesis that Cl_2 is the correct assignment of the low pH form of chlorine in solution is strengthened because the band at 538 cm^{-1} is coincident in both spectra. The observed disparity in relative band areas is simply indicative that Cl_2 in the BCS solution is much more concentrated relative to HOCl than in the ECS solution.

If equation 7 were, indeed, the correct description of the low-pH behavior of aqueous free chlorine, then minimizing the chloride ion (Cl^-) concentration in solution would diminish the formation of the potent oxidant as the pH is reduced. As described above, our commercial free-chlorine solutions (ECS) contained an equimolar amount of HOCl and Cl^-. However, we were able to prepare a stock low chloride solution (LCS) at alkaline pH using the method adapted from Reinhard and Stumm (40) as described in the Experimental Section. This LCS stock solution was diluted to 13.1 mM in free chlorine, which resulted in a Cl^- concentration of 1.12 mM. For the ECS solution at this free-chlorine concentration, the concentration of Cl^- (i.e. 13.1 mM) was more than ten times higher.

Figure 5 displays the Raman spectrum acquired from the LCS at pH 0.80 (trace B) and of the ECS at a similar pH (trace A) with the same concentration of free chlorine (i.e., 13.1 mM). It is easily seen that the ratio of band intensities in the Raman spectra at 538 to 725 cm^{-1} is much larger for the ECS solution, which contained equimolar chloride ion. Figure 6 displays the normalized band areas for the Raman bands located at 711 cm^{-1} (OCl^-) and 725 cm^{-1} (HOCl) as a function of pH for the 13.1 mM LCS sample The normalized band area of the HOCl Raman band

at 725 cm^{-1} does not exhibit a clear and consistent decrease as the pH of the solution is dropped below 5 as was observed in Figure 3 with the ECS solutions. Even at a pH below 0, there was not a significant decrease in the HOCl Raman band at 725 cm^{-1}, nor is there any significant Raman scattering observed in the 538 cm^{-1} region of the spectrum. (Note that a normalization procedure that was simpler than that described in the Experimental Section was used to construct the speciation plot in Figure 6. Because only two species were observed and both species could be completely isolated one from the other within the pH range sampled, it was acceptable to normalize each individual band area by the maximum area observed for that band.) Without chloride ion present in solution, a reverse hydrolysis reaction cannot take place if equation 7 is the correct description of the low-pH behavior. However, if equation 6 were the correct description, then lowering the chloride ion concentration should have no effect on the equilibrium towards H_2OCl^+ (equation 5). Hence all of the spectral observations lead to the conclusion that the Raman band at 538 cm^{-1} results from scattering by $Cl_2(aq)$.

Having established that equation 7 is the correct description of the low pH event, it is possible to use data from Figure 3 to estimate the concentration-based equilibrium constant K_2^{Cl2}. By rearranging equation 10, we establish that, when [HOCl] = [Cl_2]:

$$p\,K_2^{Cl2} = pH - log\ [Cl^-] \tag{17}$$

The three speciation plots in Figure 3, and the assumed chloride ion concentrations, provide three independent estimates of K_2^{Cl2}. The mean ($\pm$ sample standard deviation) of these three estimates was 2.56 ($\pm$ 1.01) x 10^{-4} M^2. However, note that this equilibrium constant should be considered an estimate only. For example, it was based on only three determinations. Also, the Cl$^-$ concentration was not confirmed by measurements in these ECS solutions. Instead, it was assumed to be equal (as stated for the commercial product) to the known free-chlorine

concentration. Furthermore, it is a concentration-based equilibrium constant. However, we note that our value is in reasonable agreement with the concentration-based value previously reported (42) of $6 \times 10^{-4}\, M^2$ for solutions with an ionic strength nearly 10 times greater than present in the solutions that we used in these experiments.

CP loss was observed in the presence of both ECS and LCS chlorine solutions over the pH range of 2-11. In the presence of ECS (Figure 1), the observed first order loss of CP increased as pH decreased from 11 to 2. The insert in Figure 1 shows the loss of CP over the pH range of 6-11. Duirk and Collette, (14) found over this pH range, that HOCl was responsible for the oxidation of CP to CPO and that OCl⁻ accelerates the hydrolysis of both CP and CPO chlorine assisted hydrolysis. Below pH 5, the observed CP loss rate greatly increased as pH decreased from 5 to 2. This increase in the observed loss rate of CP was then attributed to the formation of $Cl_2(aq)$. In the presence of LCS (Figure 7), the observed first order rate of CP loss did increase as pH decreased from 11 to 2. However, the observed rate of CP loss in the presence of LCS at low pH was not nearly as significant as it was in the presence of ECS. At pH of 2, the rate of loss of CP in LCS was about 2 orders of magnitude smaller than that observed for the ECS. However, this increase in the rate of CP loss with LCS is significant, and, in part, could be explained via the following proposed pathway. When HOCl reacts with CP, chloride ion is one of the products as well as a reduced sulfur species (S), equation 18. In the presence of excess free chlorine,

$$HOCl + CP \longrightarrow CPO + Cl^- + S + H^+ \tag{18}$$

$$4HOCl + S \longrightarrow SO_4^{2-} + 4Cl^- + 4H^+ \tag{19}$$

$$HOCl + H^+ + Cl^- \rightleftharpoons Cl_{2(aq)} + H_2O \tag{20}$$

$$Cl_2(aq) + CP \longrightarrow products \tag{21}$$

S will be rapidly oxidized to sulfate (SO_4^{2-}) resulting in four more moles of chloride for each mole of S oxidized (61), equation 19. With the presence of additional chloride ions in solution at low pH, the formation potential of $Cl_2(aq)$ is increased greatly. Therefore, the observed rate of CP loss in the presence of the LCS free chlorine solution increases due to the fact that aqueous molecular chlorine can be formed under these reaction conditions.

3.2 Loss of CP in the Presence of Bromide and Free Chlorine

The presence of bromide in drinking water sources has long been a concern of the water treatment industry because it can result in enhanced formation of potentially-hazardous DBPs under drinking water treatment conditions. Since free chlorine can rapidly oxidize bromide to hypobromous acid (HOBr) (28), it was thought that its presence might act as a catalyst in the transformation of CP during drinking water chlorination.

Initial experiments to determine if bromide does accelerate the rate of CP loss were conducted over the pH range of 7-9, [CP] = 0.5 µM, $[HOCl]_T$ = 10 and 50 µM, and increasing bromide concentrations from 0-10 µM. At $[HOCl]_T$ = 10 µM (Figure 8), plotting k_{obs} versus the bromide concentration was found to be linearly proportional to increasing bromide concentration. This was also observed at pH 8 and 9 at the higher chlorine concentration of 50 µM (Figure 9). Experiments were also conducted at pH 7 and 50 µM chlorine concentration; however, the reaction rate was too rapid to accurately quantify an observed rate of CP loss.

By comparing the slope of the regression lines at constant chlorine dose and varying pH (Table 2), the k_{obs} in the presence of bromide and free chlorine was found to be pH dependent. The pH of the solution determines the speciation of $[HOCl]_T$ between HOCl and OCl^-. Experiments conducted at lower pH have a greater percentage of $[HOCl]_T$ present as HOCl species. Since the pK_a of HOCl (7.5) is close to the pH range over which experiments are conducted, there is a large variation in the speciation of HOCl as pH increased from 7 to 9. At

24

pH 7, 8, and 9, the percentage of free chlorine present as HOCl species is approximately 75%, 23%, and 3% respectively. Since HOCl is primarily responsible for the formation of HOBr, lowering the pH increased the rate of HOBr formation and subsequently the k_{obs} for CP loss.

The formation of HOBr, due to HOCl oxidizing Br⁻, could be responsible for the increase in k_{obs} with respect to increasing bromide concentration. At the lower bromide concentrations (0.1 and 1.0 µM) and chlorine concentration of 10 µM, CP is competitive with bromide for oxidation by HOCl. Table 3 shows the rate coefficients for HOCl reacting with both CP and bromide. The reaction rate coefficient for HOCl with bromide is approximately 3 times faster than HOCl with CP. As bromide concentrations increased to 5.0 and 10.0 µM, active bromine becomes present in greater abundance than CP. Therefore, HOCl is more likely to oxidize bromide than CP when chlorine to bromide molar ratios approach 1. At low bromide concentrations and in the presence of excess free chlorine, the oxidation of CP is most likely carried out by both HOCl and HOBr. Therefore, bromide appears to act as a catalyst in the oxidation of CP by free chlorine.

While all observed rates were faster with a 50 µM chlorine concentration as compared to the analogous experiment with $[HOCl]_T = 10.0$ µM, the magnitude of bromide-catalyzed CP oxidation on k_{obs} compared to the control experiments was greater at the lower chlorine dose for pH 8 and 9. At the 10 µM chlorine concentration, addition of 10 µM of bromide induced a ~20 fold and ~30 fold increase in k_{obs} for pH 9 and 8 respectively, whereas addition of 10 µM of bromide at the 50 µM chlorine dose only increased the k_{obs} ~4 fold and 10 fold at pH 9 and 8 respectively. This indicates that the magnitude of bromide catalyzed oxidation of CP is controlled by the ratio of HOCl to bromide as well as pH. When a large excess of HOCl exists, it is the primary oxidant responsible for the loss of CP. However, when [HOCl]:[bromide] molar

ratios approach unity, HOBr becomes the primary oxidant. These two reaction scenarios are depicted schematically in Figure 10.

The relationship between k_{obs} and bromide concentration shows that increasing bromide is linearly proportional to the observed rate of CP loss in the presence of free chlorine. This result indicates that HOBr is likely the dominant oxidant responsible for CP degradation at higher bromide concentrations. The linearity of the trend also indicates that bromide acts as a catalyst in the oxidation reaction between HOCl and CP. Bromide is a catalyst in this pathway because it does not appear in the balanced equation for the reaction and after being reduced by chlorpyrifos, HOBr yields H^+ and Br^-. The regenerated bromide ion can then be re-oxidized by HOCl and participate in additional reactions with CP. The slope of the regression line for k_{obs} vs. $[Br^-]$ concentration was observed to be dependent on the concentration of free chlorine, pH, and the concentration of bromide (Table 2). All three of these parameters affect the rate of HOBr formation.

A model was developed to predict the loss of CP in the presence of free chlorine and bromide. From the stoichiometric equations in Table 3, a system of ordinary differential equations (ODEs), equations 22-28, were incorporated into a model developed to predict CP loss pathways in buffered deionized water (14). Key assumptions in this model are that HOBr will only react with CP resulting in CPO, and that all HOBr that reacts with CP results in

$$\frac{d[HOCl]_T}{dt} = -k_{HOCl,CP}[HOCl][CP] - k_{OCl,CP}[OCl^-][CP] - k_{OCl,CPO}[OCl^-][CPO] \\ - 4 * k_{HOCl,S}[HOCl][S] - k_{HOCl,Br}[HOCl][Br^-] \tag{22}$$

$$\frac{d[HOBr]_T}{dt} = k_{HOCl,Br}[HOCl][Br^-] - k_{HOBr,CP}[HOBr][CP] \tag{23}$$

$$\frac{d[Br^-]}{dt} = -k_{HOCl,Br}[HOCl][Br^-] - k_{HOBr,CP}[HOBr][CP] \tag{24}$$

$$\frac{d[S]}{dt} = k_{HOCl,CP}[HOCl][CP] + k_{HOBr,CP}[HOBr][CP] - k_{HOCl,S}[HOCl][S] \tag{25}$$

$$\frac{d[CP]}{dt} = -k_{HOCl,CP}[HOCl][CP] - k_{h,CP}[CP] - k_{OCl,CP}[OCl^-][CP] \\ - k_{HOBr,CP}[HOBr][CP] \tag{26}$$

$$\frac{d[CPO]}{dt} = k_{HOCl,CP}[HOCl][CP] - k_{h,CPO}[CPO] - k_{OCl,CPO}[OCl^-][CPO] \\ + k_{HOBr,CP}[HOBr][CP] \tag{27}$$

$$\frac{d[TCP]}{dt} = k_{h,CP}[CP] + k_{OCl,CP}[OCl^-][CP] + k_{h,CPO}[CPO] + k_{OCl,CPO}[OCl^-][CPO] \tag{28}$$

the regeneration of bromide in the aqueous system. Also, that oxidation of the reduced sulfur

species (S) can be adequately predicted by the rate coefficient determined for HOCl reaction

with sulfite (SO_3^{2-}) (61). Scientist™, an ODE solver by Micromath (Salt Lake City, UT), was

used to fit the rate coefficient for CP oxidation by hypobromous acid ($k_{HOBr,CP}$). Scientist™ uses

a modified Powell algorithm to minimize the unweighted sum of the squares of the residual error

between the predicted and experimentally observed values to estimate specific parameters in the

model.

To aid in parameter estimation, the loss of CP in the presence of HOBr was examined at

pH 6.5 (Figure 11). At this pH, over 99% of the active bromine present will be in the HOBr

form due to its pK_a of 8.8 (28). The reaction of HOBr with CP was expected to be 1 to 3 orders

of magnitude faster than HOCl with CP. This has been observed by others examining the

reactivity of HOCl and HOBr with pyrene, NOM, and sulfite (30,38,61,62). The reaction was

essentially complete after only 10 seconds. The second order rate coefficient for this reaction

was determined by nonlinear regression analysis using Sigma Plot version 8.0 (Point Richmond,

CA). The $k_{HOBr,CP}$ was found to be 1.14×10^9 M^{-1}h^{-1}, which is three orders of magnitude greater

than HOCl oxidation of CP ($k_{HOCl,CP} = 1.72 \times 10^6$ M^{-1}h^{-1}).

The system of ODEs in equations 22-28 were used to model the loss of CP in the presence of free chlorine and bromide. In Figures 12-14, model results are shown for CP loss as well as the formation of CPO and TCP at pH 8 and $[HOCl]_T = 10$, 25 and 50 μM in the absence of bromide. The model adequately predicts loss of CP and the formation of CPO and TCP. The only significant change from the model presented here verses the original model by Duirk and Collette (14) is the incorporation of oxidation of the reduced sulfur species, equation 25. Since no rate coefficients exist in literature for the oxidation of S by HOCl, it was assumed that the rate coefficient for HOCl reacting with SO_3^{2-} was sufficiently large enough to predict the loss of free chlorine due to the reaction with S. Under these experimental conditions, the model appears quite capable of predicting CP degradation pathways in the presence of free chlorine.

At pH of 8, two different sets of experiments were conducted to determine if the experimentally determined rate coefficient for $k_{HOBr,CP}$ was adequate to describe the loss of CP in the presence of bromide and free chlorine. The first set of experiments was conducted at a constant bromide concentration of 1 μM, with increasing free chlorine concentrations from 10 to 50 μM. The second set of experiments was conducted at constant free chlorine concentration of 50 μM, with increasing bromide concentrations from 1 to 10 μM. Using the experimentally determined $k_{HOBr,CP}$, CP loss was found to be significantly over-predicted for both sets of experiments. This could have been due to the fact that all active bromine being formed was assumed to only react with CP. However, HOBr does react with reduced sulfur species, such as sulfite, more rapidly than HOCl (61,62).

In the current model, all reduced sulfur species are assumed to be oxidized by HOCl and all active bromine reacts with CP. Since reaction rate coefficients for HOCl and HOBr with all the reduced sulfur species from S to SO_3^{2-} are not available in literature, it is not possible to

proportion the amount of HOBr that could potentially react with either CP or one of the reduced sulfur species. Therefore, an apparent second order rate coefficient ($k_{app\_HOBr,CP}$) was determined by pooling these data sets to predict the loss of CP in the presence of free chlorine and bromide for these experimental conditions (Figures 15-20). The $k_{app\_HOBr,CP}$ was found to be 6.01($\pm$0.40) x 10^7 $M^{-1}h^{-1}$ (95% confidence interval shown in parentheses), which is two orders of magnitude less than the experimentally determined $k_{HOBr,CP}$. Although the apparent rate coefficient is significantly smaller than the experimentally determined rate coefficient, it was able to adequately predict the loss of CP and the formation of CPO and TCP under these experimental conditions using this value for the apparent rate coefficient. Also, it still falls within the expected range of 1 to 3 orders of magnitude faster than its the chlorinated analog (61,62). The reaction with the HOBr and CP may have been too fast to be adequately captured by the experimental procedure used to investigate HOCl reactions with CP below pH of 8. This might explain, in part, the discrepancy between the experimentally determined and the apparent rate coefficients. In any event, these results indicate that active bromine pathways in the presence of OP pesticides under drinking water treatment conditions still needs to be investigated further.

3.3 *Loss of CP in the Presence of Free Chlorine and NOM*

The presence of NOM could potentially decrease the rate of CP degradation by acting as a sink for oxidants used in drinking water treatment. Conventional physical-chemical water treatment processes such as coagulation and lime softening remove a portion of the hydrophobic fraction of the NOM (63,64). More advanced water treatment processes like granular activated carbon (GAC) and membranes are capable of removing more hydrophilic NOM fractions (65). However, few community water systems employ these more advanced technologies. The ACC water treatment plant uses only conventional surface water treatment processes. Therefore, only a portion of the hydrophobic NOM fraction will be removed. Figure 21 shows the chlorine

demand studies conducted over the pH range of 7-9. Over the first half hour, approximately 12% of the free chlorine initially present is consumed by the NOM. After the initial chlorine demand of the NOM is satisfied, the loss of free chlorine attributable to reaction with NOM is relatively slow (k_{obs} = 0.012 h^{-1}) over the pH range of 7-9. These results suggest that the NOM present in the ACC water may affect the rate of CP transformation over the first half hour in the presence of free chlorine.

To examine the effect of NOM on the transformation of CP, experiments were conducted over the pH range of 7-9 and in the presence of 50 μM free chlorine. Figure 22 shows the observed first order rate of CP loss with and without the presence of NOM. In the presence of ACC NOM, the observed loss of CP was very similar to the control experiments. It appears that the conventional treatment performed at the ACC removed a portion of the hydrophobic NOM fraction that is usually associated with significant chlorine demand (36). Therefore, it might possible for the current model (developed with experiments in laboratory water) to accurately predict the transformation of CP in this low humic water.

Figures 23-27 show the experimental and model results for the loss of CP and formation of CPO and TCP in ACC water for a variety of experimental conditions. At pH 7 and 7.5 (Figures 23 and 24), the model adequately predicted CP loss and the formation of CPO and TCP. However, at these pHs, the model did slightly over-predict CP loss. This could have been due to bromide being present at 0.35 μM, but this low bromide concentration was not expected to significantly affect the rate of CP transformation (See Figures 8 and 9). On the other hand, the model performed very well predicting the formation and stability of CPO, the more toxic transformation product, as well as TCP. Over the pH range of 8-9 (Figures 25-27), the model adequately predicted the loss of CP over the experimental time frame. At pH values greater than

7.5, CPO becomes susceptible to chlorine-assisted hydrolysis due to the greater abundance of the hypochlorite ion. The model not only predicted CPO formation, but it also showed that CPO was slowly being transformed to TCP over the course of the experiment at pH 8-9. This appears to validate the ability of the model to adequately predict the loss of CP in the presence of free chlorine and NOM, as well as the ability of the model to predict the formation and stability of CPO in the presence of free chlorine.

4   CONCLUSIONS

The goal of this work was to determine the active oxidant species responsible for the degradation of CP under drinking water treatment conditions. Using Raman spectroscopy, the third species in free chlorine solutions at low pH was identified, which is responsible for the very rapid oxidation of CP at low pH. The Raman band at 538 cm^{-1} appeared as the pH of the ECS free chlorine solution was lowered and indicated the presence of a third species in addition to the hypochlorite ion and hypochlorous acid. The speciation profiles of ECS solutions at different concentrations showing variation in the low-pH "apparent pK$_a$," and disappearance of the band at 538 cm^{-1} in LCS solutions indicated that the third species in solution is Cl$_2$(aq) and not H$_2$OCl$^+$ as has been frequently assumed.

In the presence of bromide, the transformation of CP was found to be accelerated upon chlorination. HOCl rapidly oxidizes bromide to HOBr, which is a stronger oxidant. Once HOBr reacts with CP, bromide is then regenerated in the aqueous system (i.e., bromide is a catalyst increasing the rate of CP transformation). In the presence of HOBr, the reaction rate coefficient of CP with HOBr was found to be three orders of magnitude greater than the rate coefficient found for HOCl with CP. However, the experimentally determined rate coefficient was found to be too large to accurately predict the loss of CP and the formation of CPO and TCP under the experimental conditions used in this study. An apparent second order rate coefficient (k$_{app\_HOBr,CP}$), which was two orders of magnitude less than the experimentally determined rate coefficient, was found to adequately fit the experimental results. This was assumed to be due to HOBr reacting with not only CP but with reduced sulfur species evolving from the initial oxidation of CP by either HOCl or HOBr. Future work will be done to further elucidate active bromine pathways in the presence of free chlorine and CP.

The role of NOM on the transformation of CP was investigated using Athens-Clarke County water, which was collected prior to chlorination. Under the experimental conditions used in this study, the established model, initially developed to predict the transformation pathways of CP in laboratory water, was found to adequately predict the loss of CP and the formation of CPO and TCP in the ACC water. It was assumed that due to the low humic content of the ACC water, the chlorine demand that was exerted by the NOM was not sufficient to significantly affect the rate of CP transformation. Also, the model was able to predict the formation and stability of CPO over the entire pH range. In waters that are low in aquatic humic substances, the model appears to adequately predict CP transformation pathways.

The work presented here shows the application of a model, developed to predict the loss of CP in buffered aqueous systems, to predict the loss of CP over a greater range of conditions that are more closely associated with drinking water treatment. However, the need still exists to systematically investigate chlorination of OP pesticides as a class and determine if reactivity with aqueous chlorine is related in a predictable way to OP chemical structure. If a relationship between reactivity and pesticide structure exists, the ability to predict the fate of OP pesticides in the presence of free chlorine would greatly aid regulators in assuring that tolerances to OP pesticide exposure from drinking water are not exceeded. After developing predictive tools for the entire class of OP pesticides, we plan to address other important classes of pesticides and toxic chemicals.

5 REFERENCES

(1)   Kolpin, D. W.; Barbash, J. E.; Gilliom, R. J. Pesticides in ground water of the United States, 1992-1996. *Ground Water* **2000**, *38*, 858-863.

(2)   Verstraeten, I. M.; Thurman, E. M.; Lindsey, M. E.; Lee, E. C.; Smith, R. D. Changes in concentrations of triazine and acetamide herbicides by bank filtration, ozonation, and chlorination in a public water supply. *Journal of Hydrology* **2003**, *276*, 287-288.

(3)   Coupe, R. H.; Blomquist, J. D. Water-soluble pesticides in finished water of community water supplies. *Journal American Water Works Association* **2004**, *96*, 56-68.

(4)   *Community Water System Survey*; United States Environmental Protection Agency, 1997; Vol. 1, EPA 815-R-97-011a.

(5)   Lopez, A.; Mascolo, G.; Tiravanti, G.; Santori, M.; Passino, R. Oxidation of Sulfur-Containing S-Triazines During Groundwater Hypochlorination. *Water Science and Technology* **1994**, *30*, 53-59.

(6)   Mascolo, G.; Lopez, A.; Passino, R.; Ricco, G.; Tiravanti, G. Degradation of Sulfur-Containing S-Triazines During Water Chlorination. *Water Research* **1994**, *28*, 2499-2506.

(7)   Adams, C. D.; Randtke, S. J. Removal of Atrazine from Drinking-Water by Ozonation. *Journal American Water Works Association* **1992**, *84*, 91-102.

(8)   Miles, C. J. Degradation of Aldicarb, Aldicarb Sulfoxide, and Aldicarb Sulfone in Chlorinated Water. *Environmental Science & Technology* **1991**, *25*, 1774-1779.

(9)   Mason, Y. Z.; Choshen, E.; Ravacha, C. Carbamate Insecticides - Removal from Water by Chlorination and Ozonation. *Water Research* **1990**, *24*, 11-21.

(10)   Kodama, S.; Yamamoto, A.; Matsunaga, A. S-Oxygenation of thiobencarb in tap water processed by chlorination. *Journal of Agricultural and Food Chemistry* **1997**, *45*, 990-994.

(11)   Zhang, Q.; Pehkonen, S. O. Oxidation of diazinon by aqueous chlorine: Kinetics, mechanisms, and product studies. *Journal of Agricultural and Food Chemistry* **1999**, *47*, 1760-1766.

(12)   Magara, Y.; Aizawa, T.; Matumoto, N.; Souna, F. Degradation of Pesticides by Chlorination During Water-Purification. *Water Science and Technology* **1994**, *30*, 119-128.

(13)   Wu, J. G.; Laird, D. A. Abiotic transformation of chlorpyrifos to chlorpyrifos oxon in chlorinated water. *Environmental Toxicology and Chemistry* **2003**, *22*, 261-264.

(14)   Duirk, S. E.; Collette, T. W. Degradation of Chlorpyrifos in Aqueous Chlorine Solutions: Pathways, Kinetics, and Modeling. *Environmental Science and Technology* **2006**, *40*, 546-551.

(15)   Deborde, M.; Rabouan, S.; Gallard, H.; Legube, B. Aqueous chlorination kinetics of some endocrine disruptors. *Environmental Science & Technology* **2004**, *38*, 5577-5583.

(16)   Gallard, H.; Von Gunten, U. Chlorination of Phenols: Kinetics and Formation of Chloroform. *Environmental Science & Technology* **2002**, *36*, 884-890.

(17)   Rule, K. L.; Ebbert, V. R.; Vikesland, P. J. Formation of Chloroform and Chlorinated Organics by Free-Chlorine-Mediated Oxidation of Triclosan. *Environmental Science and Technology* **2005**, *39*, 3176-3185.

(18)   Rebenne, L. M.; Gonzalez, A. C.; Olson, T. M. Aqueous chlorination kinetics and mechanism of substituted dihydroxybenzenes. *Environmental Science & Technology* **1996**, *30*, 2235-2242.

(19)   Arotsky, J.; Symons, M. C. R. Halogen Cations. *Quarterly Reviews of the Chemical Society* **1962**, *16*, 282-297.

(20)   Donaldson, D. J.; Ravishankara, A. R.; Hanson, D. R. Detailed Study of HOCl + HCl -> Cl2 + H2O in Sulfuric Acid. *Journal of Physical Chemistry A* **1997**, *101*, 4717-4725.

(21)   Liu, D. K.; Chang, S.-G. Removal of Nitric Oxide from Flue Gas Using Water-Soluble Iron(II) Dithiocarbamates. *Environmental Science Technology* **1988**, *22*, 1196-2000.

(22)   Swain, C. G.; Crist, D. R. Mechanisms of Chlorination by Hypochlorous Acid. The Last of the Chloronium Ion, Cl+. *Journal of the American Chemical Society* **1972**, *94*, 3195-3200.

(23)   Swain, C. G.; Ketley, A. D. The Chloronium Ion as an Intermediate in Chlorination of Aromatic Compounds by Hypochlorous Acid. *Journal of the American Chemical Society* **1955**, *77*, 3410.

(24)   Saha, B.; Stanbury, D. M. Oxidation of [Ru(NH3)5isn](BF4)2 by Hypochlorous Acid and Chlorine in Aqueous Acidic Media. *Inorganic Chemistry* **2001**, *40*, 5139-5146.

(25)   Cooper, J. N.; Margerum, D. W. Kinetics and mechanism of the oxidation of hydroxylamine by aqueous chlorine *Inorganic Chemistry* **1993**, *32*, 5905-5910.

(26)   Dowell, C. T. The Action of Chlorine Upon Hydrazine, Hydroxylamine and Urea. *Journal of the American Chemical Society* **1919**, *41*, 124-125.

(27)   Siddiqui, M. S.; Amy, G. L.; Rice, R. G. Bromate Ion Formation - a Critical-Review. *Journal American Water Works Association* **1995**, *87*, 58-70.

(28)   Kumar, K.; Margerum, D. W. Kinetics and Mechanism of General-Acid-Assisted Oxidation of Bromide by Hypochlorite and Hypochlorous Acid. *Inorganic Chemistry* **1987**, *26*, 2706-2711.

(29)   Bousher, A.; Brimblecombe, P.; Midgley, D. Rate of Hypobromite Formation in Chlorinated Seawater. *Water Research* **1986**, *20*, 865-870.

(30)   Hu, J. Y.; Jin, X. H.; Kunikane, S.; Terao, Y.; Aizawa, T. Transformation of pyrene in aqueous chlorination in the presence and absence of bromide ion: Kinetics, products, and their aryl hydrocarbon receptor-mediated activities. *Environmental Science & Technology* **2006**, *40*, 487-493.

(31)   Pourmoghaddas, H.; Stevens, A. A. Relationship between Trihalomethanes and Haloacetic Acids with Total Organic Halogen During Chlorination. *Water Research* **1995**, *29*, 2059-2062.

(32)   Pourmoghaddas, H.; Stevens, A. A.; Kinman, R. N.; Dressman, R. C.; Moore, L. A.; Ireland, J. C. Effect of Bromide Ion on Formation of Haas During Chlorination. *Journal American Water Works Association* **1993**, *85*, 82-87.

(33)   Singer, P. C. Humic substances as precursors for potentially harmful disinfection by-products. *Water Science and Technology* **1999**, *40*, 25-30.

(34)   Westerhoff, P.; Siddiqui, M. S.; Debroux, J.; Zhai, W.; Ozekin, K.; Amy, G. *Nation-wide Bromide Occurence and Bromate Formation Potential in Drinking Water Supplies*; Amreican Society of Civil Engineers: Salem, MA, 1994.

(35)   Thurman, E. M. *Organic geochemistry of natural waters*; Junk Publishers: Boston, MA, 1985.

(36)   Najm, I. N.; Patania, N. L.; Jacangelo, J. G.; Krasner, S. W. Evaluating Surrogates for Disinfection by-Products. *Journal American Water Works Association* **1994**, *86*, 98-106.

(37) Reckhow, D. A.; Singer, P. C.; Malcolm, R. L. Chlorination of Humic Materials - by-Product Formation and Chemical Interpretations. *Environmental Science & Technology* **1990**, *24*, 1655-1664.

(38) Westerhoff, P.; Chao, P.; Mash, H. Reactivity of natural organic matter with aqueous chlorine and bromine. *Water Research* **2004**, *38*, 1502-1513.

(39) *Standard Methods for the Examination of Water and Wastewater*; 20th ed.; APHA, AWWA and WEF: Washington D. C., 1998.

(40) Reinhard, M.; Stumm, W. Kinetics of Chlorination of p-Xylene in Aqueous Solution. In *Water Chlorination: Chemistry, Environmental Impact, and Health Effects*; Jolley, R. L., Ed.; Lewis Publishers: Ann Arbor, 1980; Vol. 3, pp 209-218.

(41) Leaist, D. G. Absorption of Chlorine into Water. *Journal of Solution Chemistry* **1986**, *15*, 827-838.

(42) Eigen, M.; Kustin, K. The Kinetics of Halogen Hydrolysis. *Journal of the American Chemical Society* **1962**, *84*, 1355-1361.

(43) Lifshitz, A.; Perlmutter-Hayman, B. The Kinetics of the Hydrolysis of Chlorine. I. Reinvestigation of the Hydrolysis in Pure Drinking Water. *Journal of Physical Chemistry* **1960**, *64*, 1663-1665.

(44) Wang, T. X.; Margerum, D. W. Kinetics of Reversible Chlorine Hydrolysis - Temperature-Dependence and General Acid Base-Assisted Mechanisms. *Inorganic Chemistry* **1994**, *33*, 1050-1055.

(45) Aieta, E. M.; Roberts, P. V. Application of Mass-Transfer Theory to the Kinetics of a Fast Gas-Liquid Reaction: Chlorine Hydrolysis. *Environmental Science & Technology* **1986**, *20*, 44-50.

(46) Connick, R. E. The Interaction of Hydrogen Peroxide and Hypochlorous Acid in Acidic Solutions Containing Chloride Ion. *Journal of the American Chemical Society* **1947**, *69*, 1509-1513.

(47) Connick, R. E.; Chia, Y.-T. The Hydrolysis of Chlorine and its Variation with Temperature. *Journal of the American Chemical Society* **1959**, *81*, 1280-1283.

(48) Gershenzon, M.; Davidovits, P.; Jayne, J. T.; Kolb, C. E.; Worsnop, D. R. Rate Constant for the Reaction of Cl2 (aq) with OH-. *Journal of Physical Chemistry A* **2002**, *106*, 7748-7754.

(49) Lifshitz, A.; Perlmutter-Hayman, B. The Kinetics of the Hydrolysis of Chlorine. II. The Hydrolysis in the Presence of Acetate. *Journal of Physical Chemistry* **1961**, *65*, 753-757.

(50) Lifshitz, A.; Perlmutter-Hayman, B. The Kinetics of the Hydrolysis of Chlorine. III. The Reaction in the Presence of Various Bases and a Discussion of the Mechanism. *Journal of Physical Chemistry* **1962**, *66*, 701-705.

(51) Rehfeld, B. M.; Pratt, D. E. Influence of Organophosphate Insecticides on Ascorbic Acid Oxidation in Aqueous Systems. *Journal of Food Science* **1969**, *34*, 551-&.

(52) Everall, N.; Owen, H.; Slater, J. Performance Analysis of an Integrated Process Raman Analyzer Using a Multiplexed Transmission Holographic Grating, CCD Detection, and Confocal Fiberoptic Sampling. *Applied Spectroscopy* **1995**, *49*, 610-615.

(53) Williams, T. L.; Martin, R. B.; Collette, T. W. Raman Spectroscopic Analysis of Fertilizers and Plant Tissue for Perchlroate. *Applied Spectroscopy* **2001**, *55*, 967-988.

(54) Collette, T. W.; Williams, T. L.; D'Angelo, J. C. Optimization of Raman Spectroscopy for Speciation of Organics in Water. *Applied Spectroscopy* **2001**, *55*, 750 - 766.

(55) Liu, B.; McConnell, L. L.; Torrents, A. Hydrolysis of chlorpyrifos in natural waters of the Chesapeake Bay. *Chemosphere* **2001**, *44*, 1315-1323.

(56) Hu, J. Y.; Morita, T.; Magara, Y.; Aizawa, T. Evaluation of reactivity of pesticides with ozone in water using the energies of frontier molecular orbitals. *Water Research* **2000**, *34*, 2215-2222.

(57) Kolpin, D. W.; Furlong, E. T.; Meyer, M. T.; Thurman, E. M.; Zaugg, S. D.; Barber, L. B.; Buxton, H. T. Pharmaceuticals, hormones, and other organic wastewater contaminants in US streams, 1999-2000: A national reconnaissance. *Environmental Science & Technology* **2002**, *36*, 1202-1211.

(58) Nakagawara, S.; Goto, T.; Nara, M.; Ozawa, Y.; Hotta, K.; Arata, Y. Spectroscopic Characterization and the pH Dependence of Bactericidal Activity of the Aqueous Chlorine Solution. *Analytical Sciences* **1998**, *14*, 691-698.

(59) Snoeyink, V. L.; Jenkins, D. A. *Water Chemistry*; John Wiley & Sons: New York, NY, 1980.

(60) Skoog, D. A.; West, D. M. In *Fundamentals of Analytical Chemistry*; 2nd ed.; Holt, Reinhart and Winston, Inc.: New York, 1969; pp 294-297.

(61) Fogelman, K. D.; Walker, D. M.; Margerum, D. W. Non-Metal Redox Kinetics - Hypochlorite and Hypochlorous Acid Reactions with Sulfite. *Inorganic Chemistry* **1989**, *28*, 986-993.

(62) Troy, R. C.; Margerum, D. W. Nonmetal Redox Kinetics - Hypobromite and Hypobromous Acid Reactions with Iodide and with Sulfite and the Hydrolysis of Bromosulfate. *Inorganic Chemistry* **1991**, *30*, 3538-3543.

(63) Bob, M.; Walker, H. W. Lime-soda softening process modifications for enhanced NOM removal. *Journal of Environmental Engineering-Asce* **2006**, *132*, 158-165.

(64) Crozes, G.; White, P.; Marshall, M. Enhance Coagulation - Its Effect on Nom Removal and Chemical Costs. *Journal American Water Works Association* **1995**, *87*, 78-89.

(65) Jacangelo, J. G.; Demarco, J.; Owen, D. M.; Randtke, S. J. Selected Processes for Removing Nom - an Overview. *Journal American Water Works Association* **1995**, *87*, 64-77.

(66) Macalady, D. L.; Wolfe, N. L. New Perspectives on the Hydrolytic Degradation of the Organophosphorothioate Insecticide Chlorpyrifos. *Journal of Agricultural and Food Chemistry* **1983**, *31*, 1139-1147.

TABLES

Table 1   NOM and source water characteristics for the ACC water collected prior to
             chlorination.

Source	SUVA$_{254}$ (L/m-mg)	SUVA$_{280}$ (L/m-mg)	[a][NH$_3$]$_T$ (μM)	[Cl$^-$] (μM)	[NO$_2^-$] (μM)	[Br$^-$] (μM)	[b][PO$_4$]$_T$ (μM)	[SO$_4^{2-}$] (μM)
ACC	1.61	1.07	2.06	93.46	0.04	0.35	[c]ND	8.30

[a][NH3]$_T$ = [NH$_4^+$] + [NH$_3$]
[b][PO$_4$]$_T$ = [H$_3$PO$_4$] + [H$_2$PO$_4^-$] + [HPO$_4^{2-}$] + [PO$_4^{3-}$]
[c]ND = Non-detect

Table 2   The slopes of k_{obs} vs. [Br$^-$] for each pH and [HOCl] concentration.

pH	[HOCl] (μM)	k_{obs} (h^{-1}) vs. [Br$^-$]
7	10	10.3
8	10	2.7
9	10	0.4
8	50	5.3
9	50	0.6

Table 3   Stoichiometric equations and rate coefficients used in the chlorpyrifos degradation pathway model.

Reaction Stoichiometry	Rate/Equilibrium Coefficient (25 °C)	Reference
1 $HOCl + CP \xrightarrow{k_r} CPO + H^+ + Cl^- + S$	$k_{HOCl,CP} = 1.72 \times 10^6 \ M^{-1}h^{-1}$	(14)
2 $4HOCl + S \xrightarrow{k_{HOCl,S}} 4H^+ + 4Cl^- + SO_4^{2-}$	$k_{HOCl,S} = 2.74 \times 10^{12} \ M^{-1}h^{-1}$	(61)
3 $HOCl + Br^- \xrightarrow{k_{HOCl,Br}} HOBr + Cl^-$	$k_{HOCl,Br} = 5.6 \times 10^6 \ M^{-1}h^{-1}$	(28)
4 $HOBr + CP \xrightarrow{k_{HOBr,CP}} CPO + H^+ + Cl^-$	$k_{HOBr,CP}$ = see text	This work
5 $CP \xrightarrow{k_{h,CP}} TCP$	$k_{h,CP} = k_{N,CP} + k_{B,CP}[OH^-]$ $k_{N,CP} = 3.72 \times 10^{-4} \ h^{-1}$ $k_{B,CP} = 37.0 \ M^{-1}h^{-1}$	(66)
6 $CPO \xrightarrow{k_{h,CPO}} TCP$	$k_{h,CPO} = k_{N,CPO} + k_{B,CPO}[OH^-]$ $k_{N,CPO} = 2.13 \times 10^{-3} \ h^{-1}$ $k_{B,CPO} = 230 \ M^{-1}h^{-1}$	(14)
7 $CP + OCl^- \xrightarrow{k_{OCl,CP}} TCP + Cl^-$	$k_{OCl,CP} = 990 \ M^{-1}h^{-1}$	(14)
8 $CPO + OCl^- \xrightarrow{k_{OCl,CPO}} TCP + Cl^-$	$k_{OCl,CPO} = 1340 \ M^{-1}h^{-1}$	(14)
9 $HOCl \rightleftharpoons H^+ + OCl^-$	$pK_a = 7.5$	(59)

FIGURES
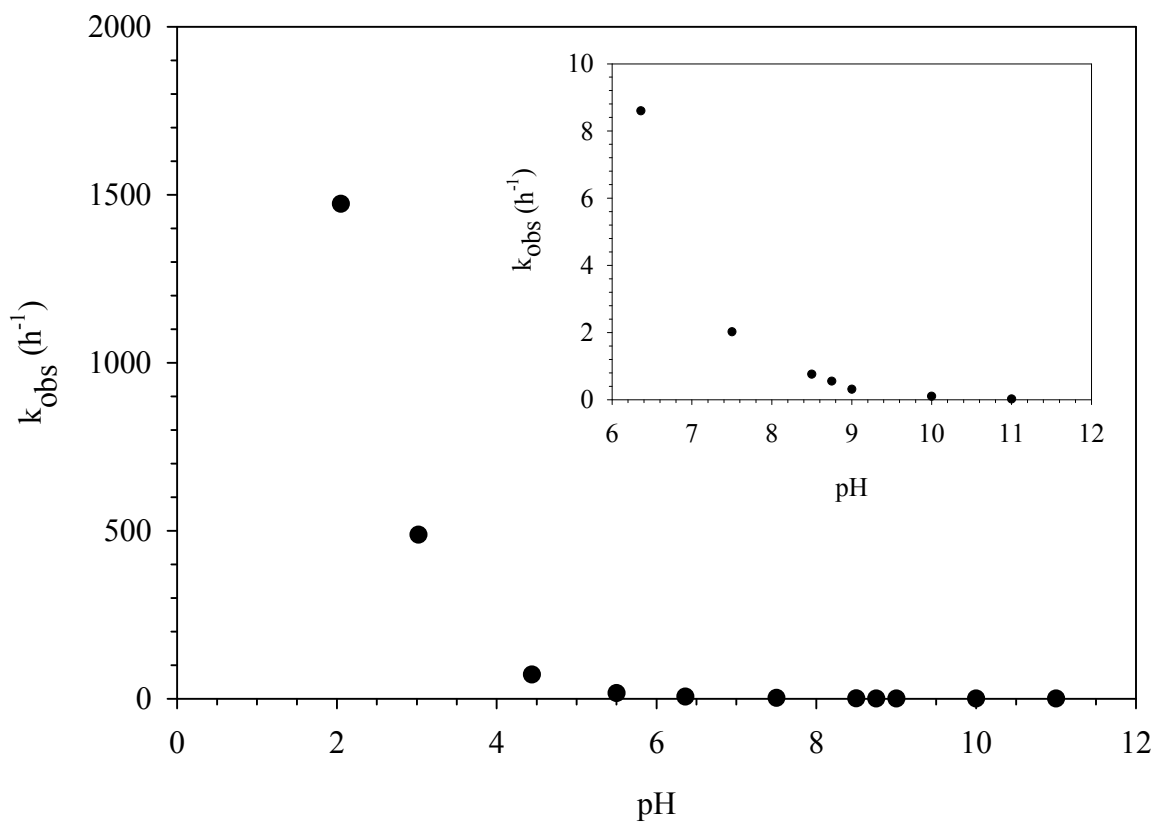
Figure 1   Observed first order loss rate coefficients for chlorpyrifos over the pH range of 2-11 in the presence of ECS. $[CP]_o = 0.5$ μM, $[Buffer]_T = 10$ mM, Temperature = $25\pm1°C$, and $[HOCl]_T = 10$ μM.
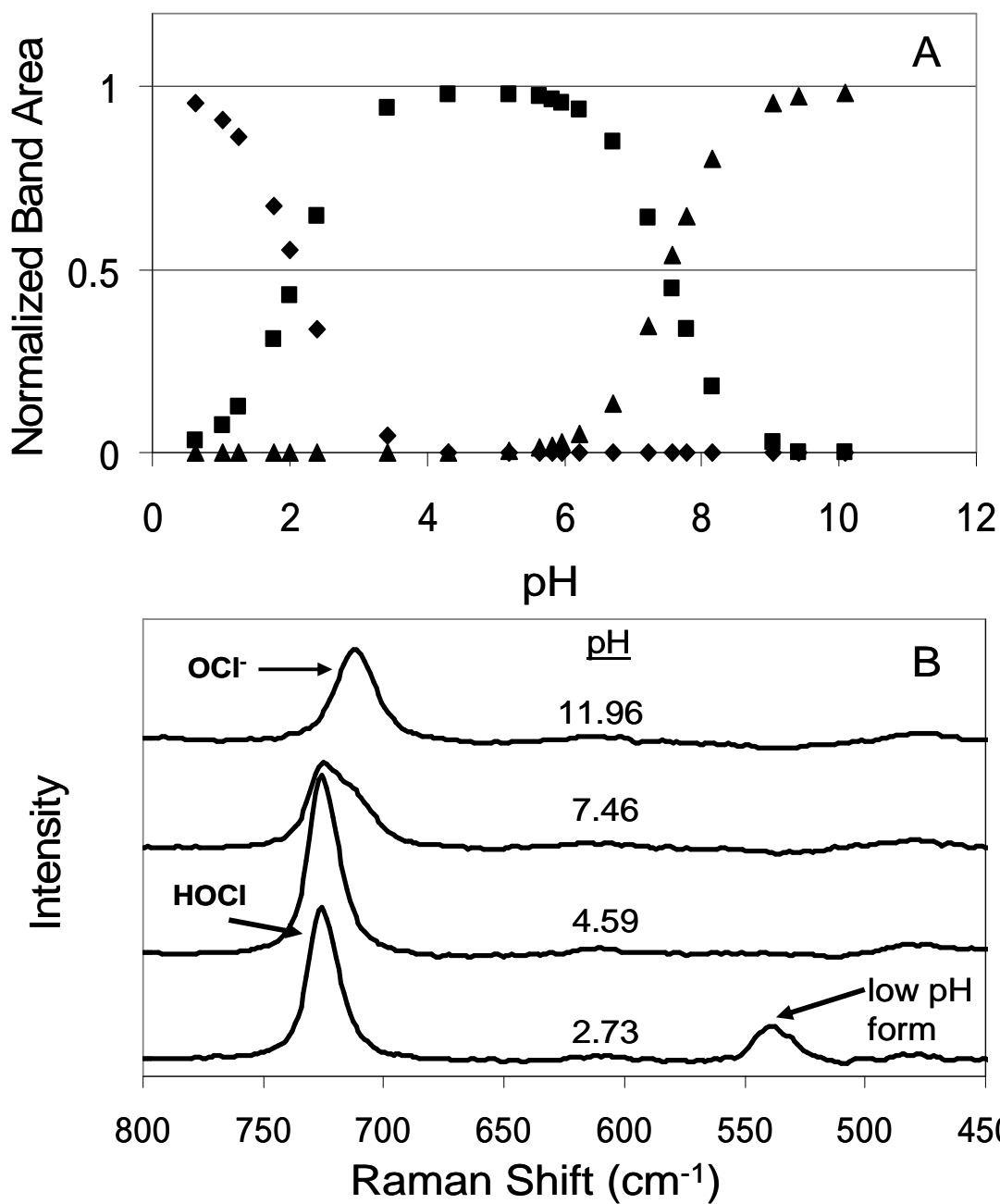
Figure 2   (A.) Speciation plot of the 26.2 mM commercial free chlorine solution (the ECS solution) generated by monitoring the normalized areas of the Raman bands from OCl⁻ at 711 cm-1 (▲), HOCl at 725 cm-1(■) and the low pH species at 538 cm^{-1} (♦). (B.) Background-subtracted Raman spectra of ECS solutions. The OCl⁻ band is observed in the top two spectra and the HOCl band is observed in the bottom three spectra. An additional band for the low pH form appears as the pH is lowered below 5.
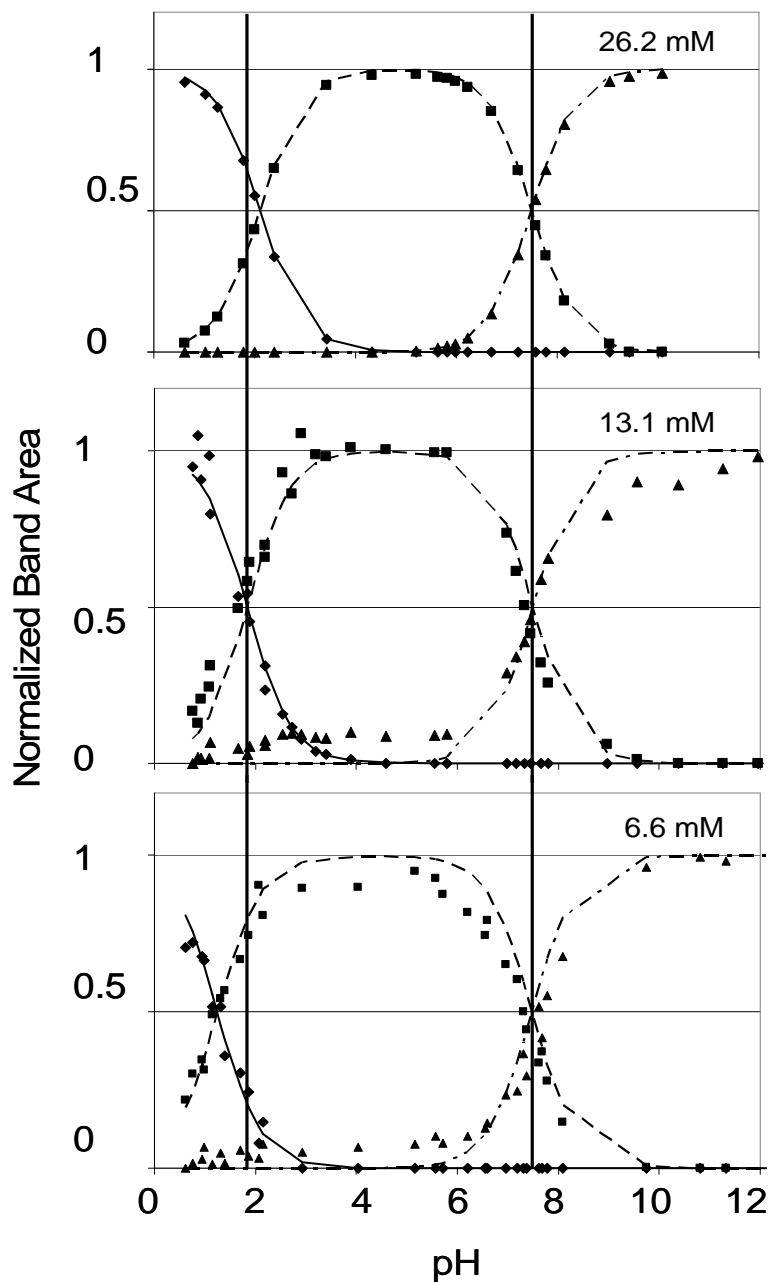
Figure 3   Speciation plots of commercial free chlorine solutions (ECS solutions) generated by monitoring the normalized areas of the Raman bands from OCl⁻ at 711 cm-1 (▲, dash-dot model line), HOCl at 725 cm-1 (■, dashed model line) and the low pH species at 538 cm^{-1} (♦, solid model line). Vertical lines indicate the apparent pKₐs at 13.1 mM. The pKa for the protonation of OCl⁻ to HOCl occurs at 7.50 for all three concentrations. The apparent pK at lower pH varies from (from top to bottom): 2.11, 1.84, and 1.25.
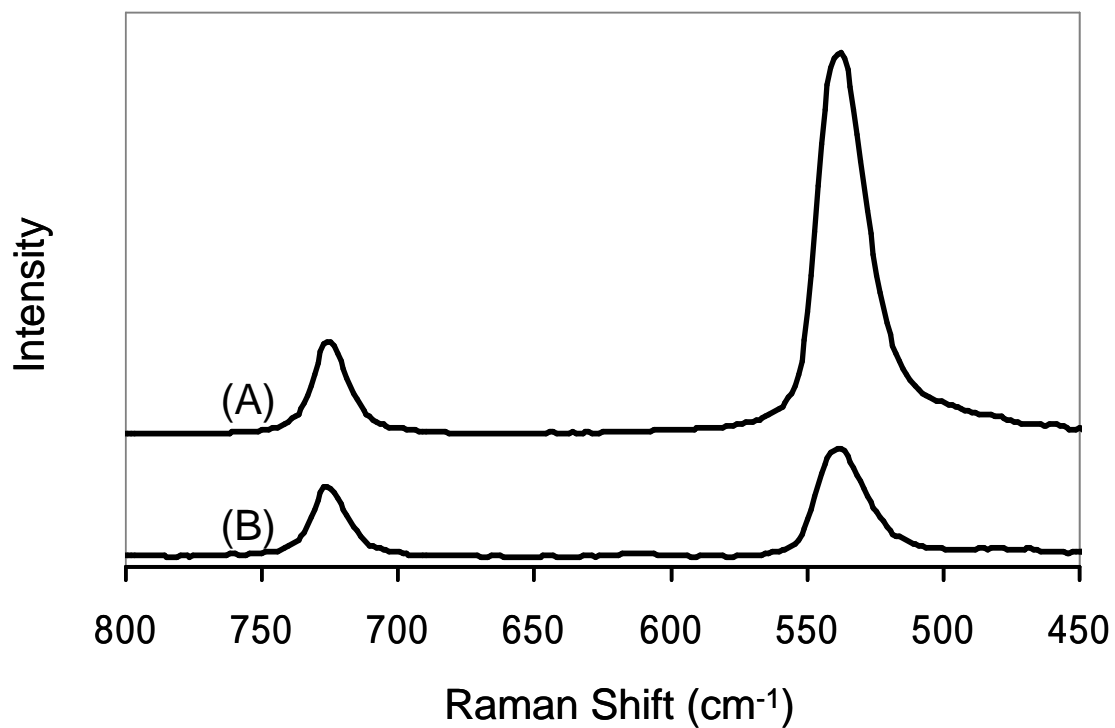
Figure 4   Raman spectrum acquired from (A) a buffered aqueous solution at pH 1.45 through which chlorine gas was bubbled (BCS) and (B) a pH 1.63 solution containing 13.1 mM commercial free chlorine (ECS). The band at 538 cm^{-1} is due to the presence of Cl_2 (aq) in each solution.
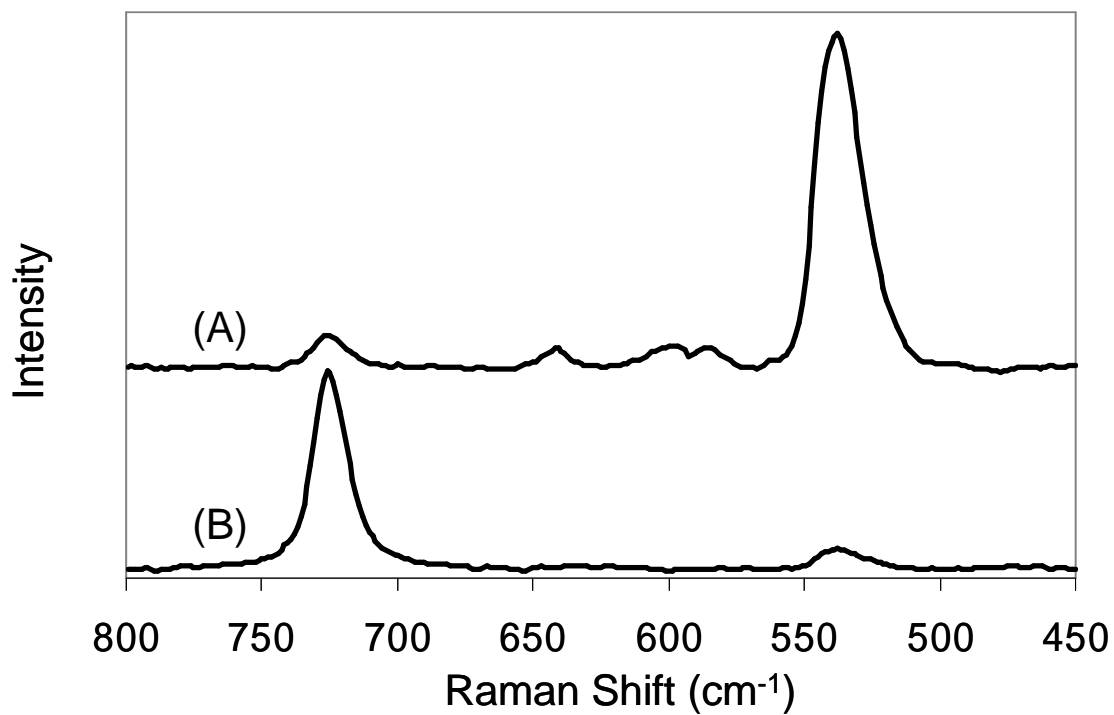
Figure 5   Raman spectra comparing 13.1 mM free chlorine solutions with (A) equimolar chloride ion at pH 0.75 (ECS) and (B) free chlorine solution with reduced chloride ion at pH 0.80 (LCS). The spectrum of the solution containing equimolar chloride ion has a much larger band at 538 cm^{-1} (due to aqueous Cl_2) than the solution with greatly reduced chloride concentration.
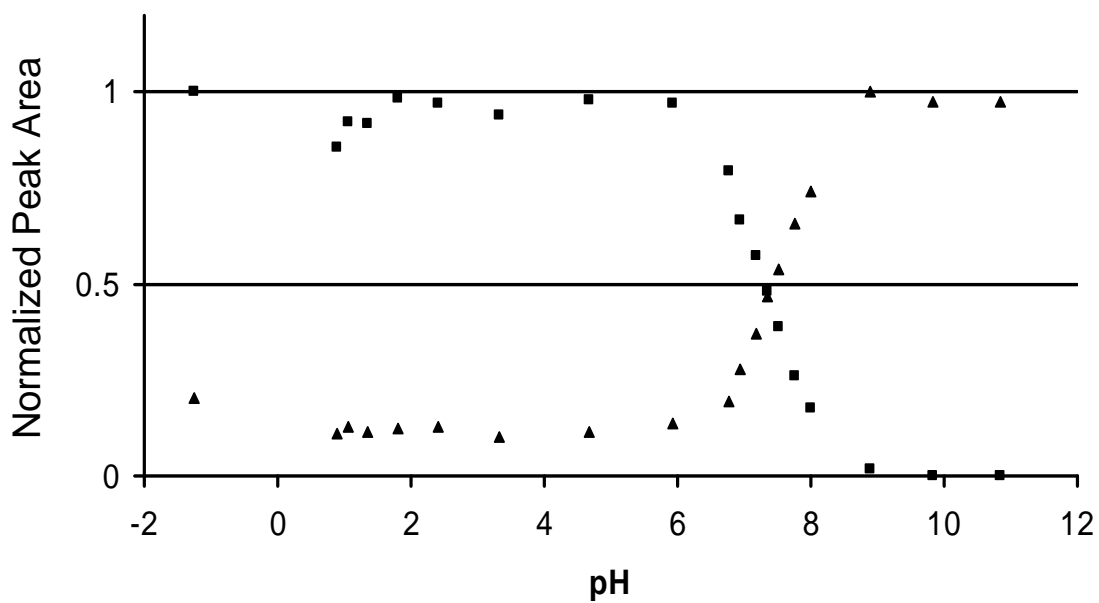
Figure 6   Speciation profile of the LCS free chlorine solution with reduced chloride ion concentration generated by monitoring the normalized areas of the Raman bands from HOCl at 725 cm-1 (■) and OCl⁻ at 711 cm-1 (▲). The predominant species in solution at low pH remains HOCl throughout, and a significant drop in its total area is not observed as pH decreases.
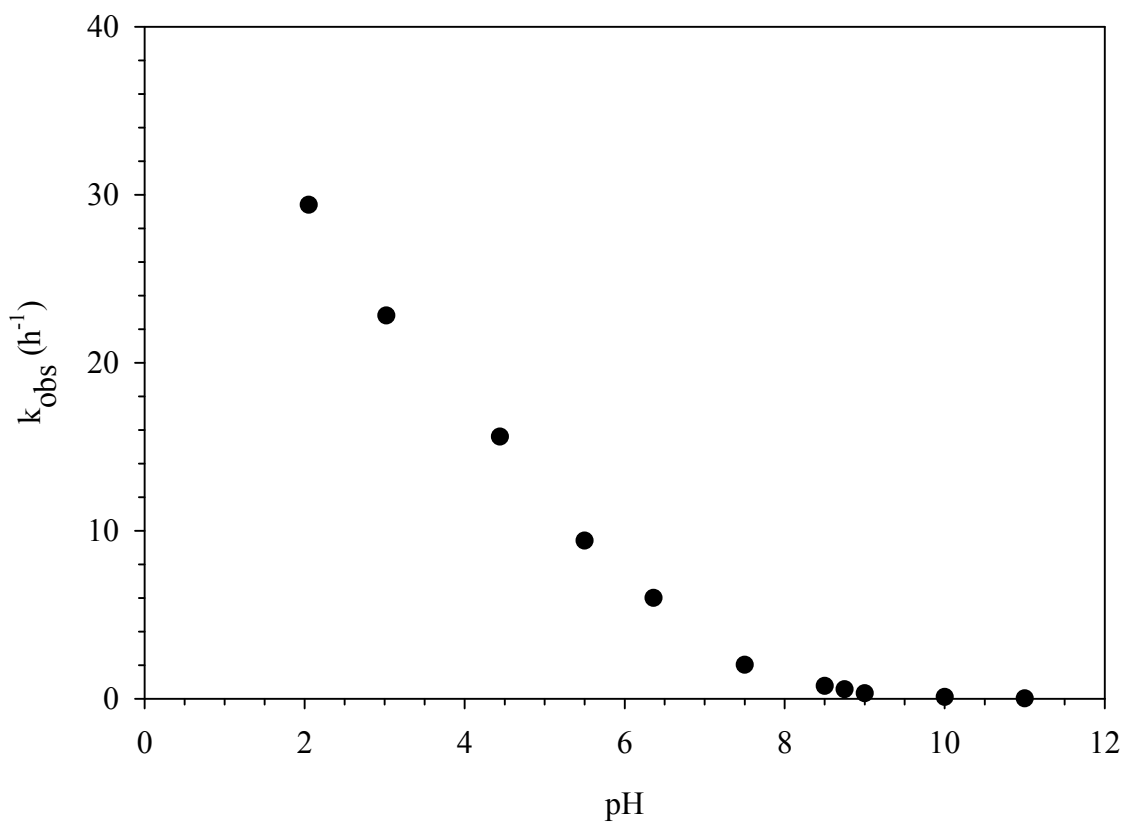
Figure 7   Observed first order loss rate coefficients for chlorpyrifos over the pH range of 2-11 in the presence of LCS. $[CP]_o = 0.5\ \mu M$, $[Buffer]_T = 10\ mM$, Temperature = $25 \pm 1°C$, and $[HOCl]_T = 10\ \mu M$.
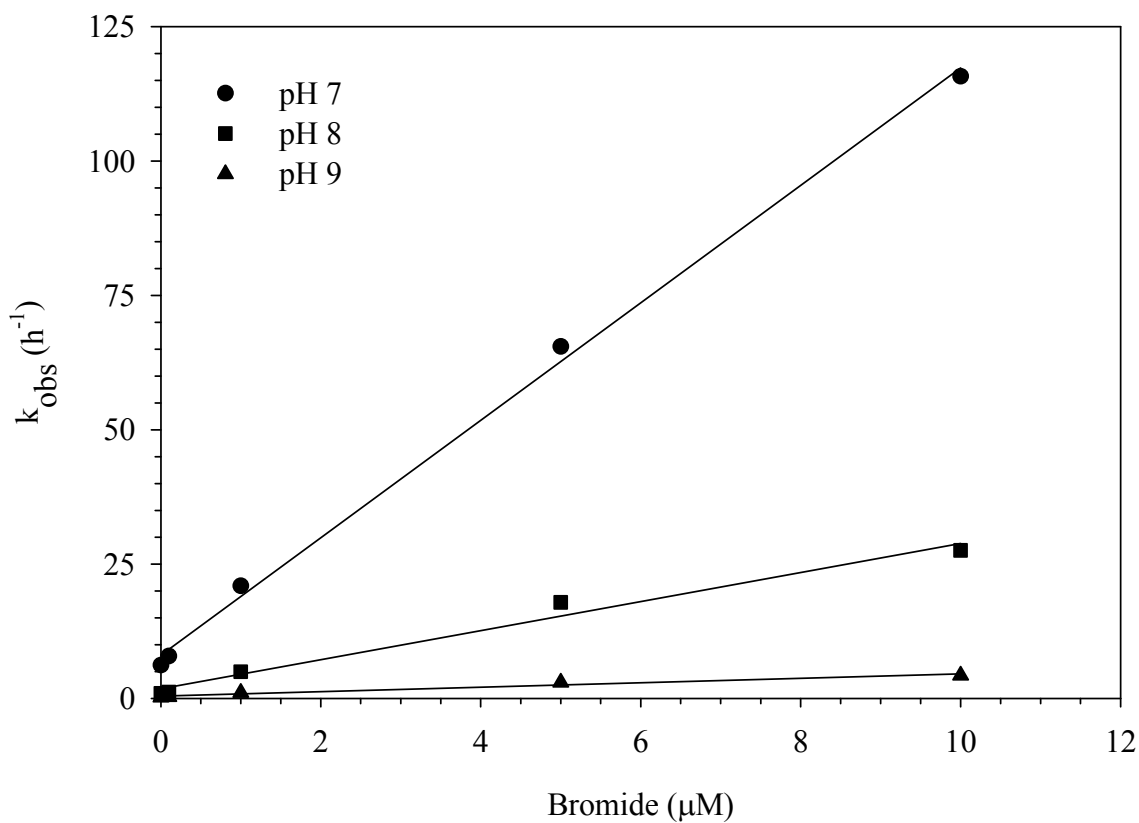
Figure 8   Observed first order rate coefficients for CP loss in the presence of increasing bromide concentrations at $[HOCl]_T = 10$ μM over the pH range of 7-9. $[CP]_o = 0.5$ μM, $[Buffer]_T = 10$ mM, and Temperature = 25 °C.
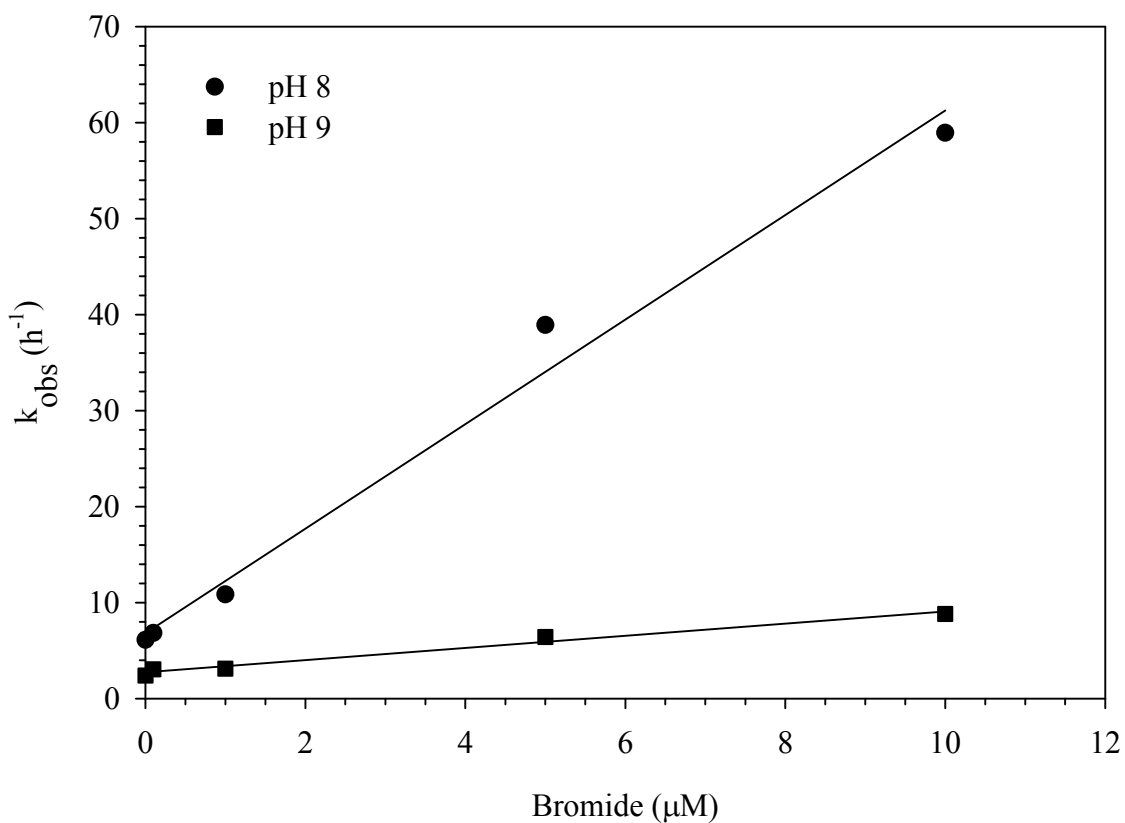
Figure 9   Observed first order rate coefficients for CP loss in the presence of increasing bromide concentrations at $[HOCl]_T = 50$ μM at pH 8 and 9. $[CP]_o = 0.5$ μM, $[Buffer]_T = 10$ mM, and Temperature = 25 °C.
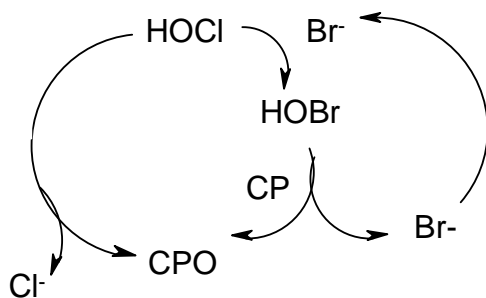
Figure 10   Two possible oxidation pathways for CP at high and low [HOCl]:[Br⁻] ratios. The pathway on the left shows the predominant pathway when [HOCl]≫[Br⁻] and the pathway on the right shows the predominant pathway when [HOCl]:[Br⁻] approaches 1.
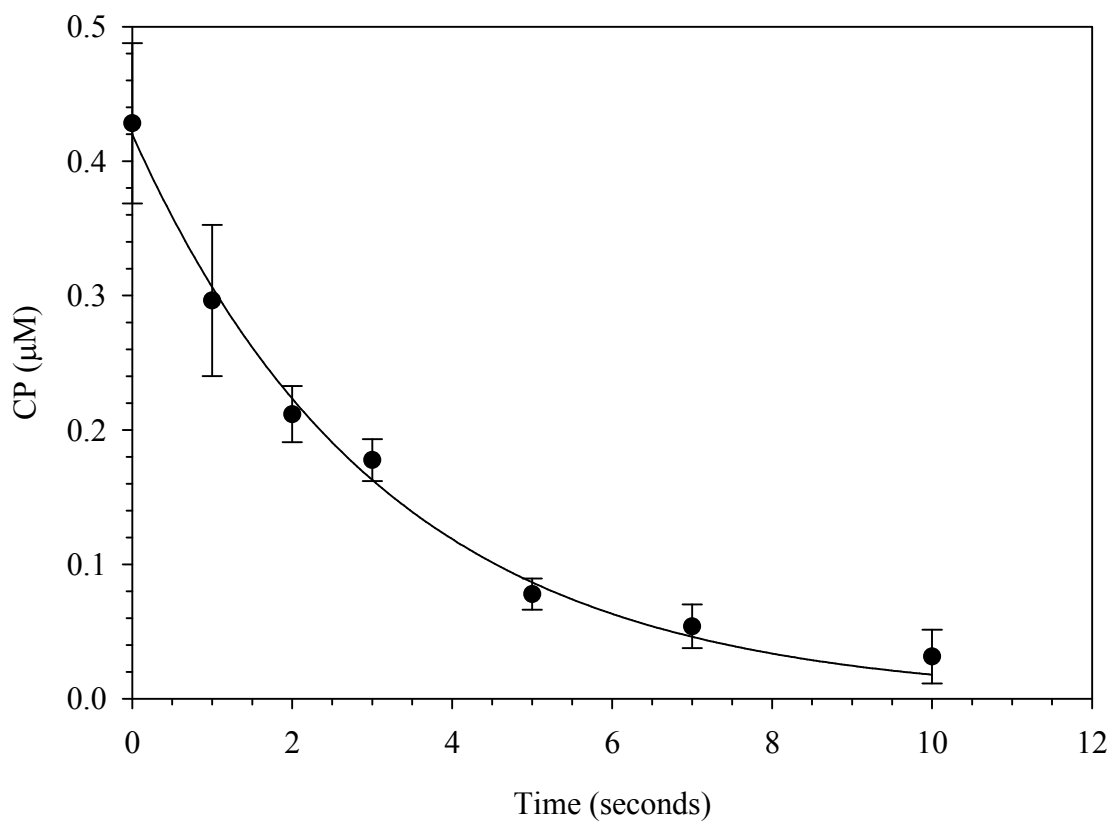
Figure 11   Loss of CP in the presence of hypobromous acid at pH 6.5. $[CP]_o = 0.42$ μM, $[HOBr]_T = 10$ μM, $[Buffer]_T = 10$ mM, and Temperature = 25 °C.
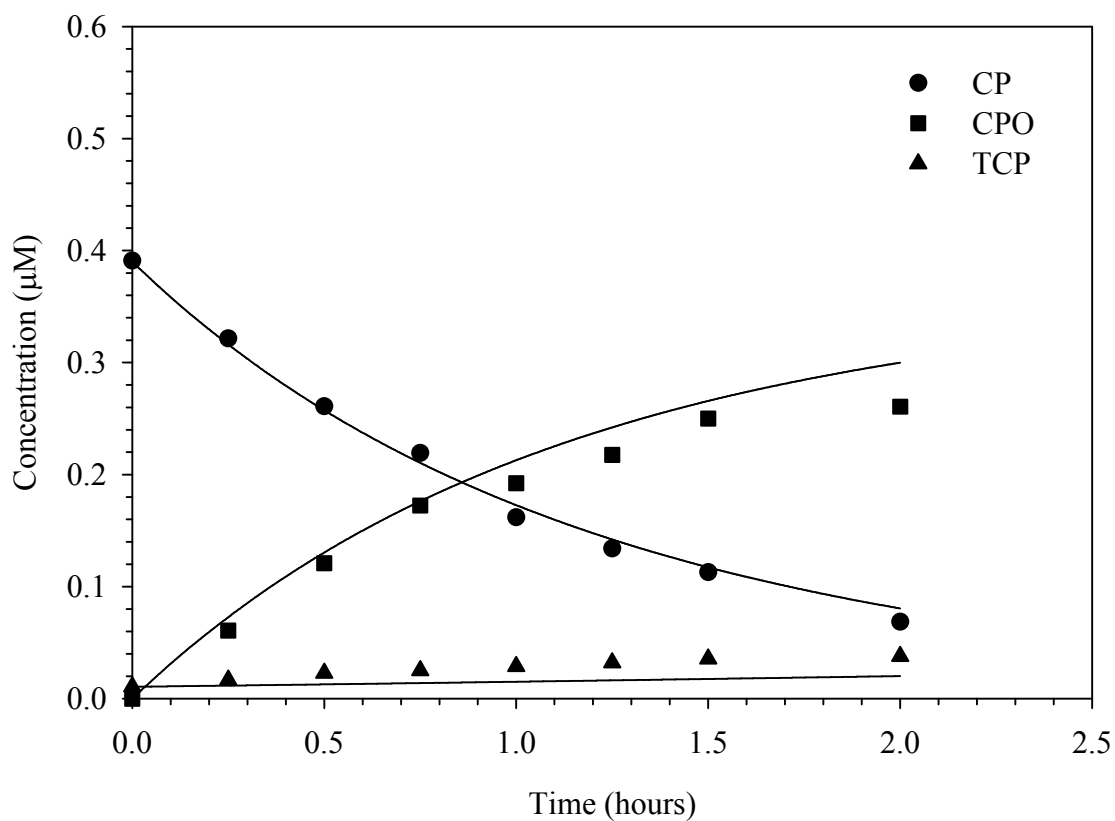
Figure 12   CP degradation in the presence of free chlorine at pH 8.0 in the absence of bromide. $[CP]_o = 0.39$ μM, $[HOCl]_T = 10$ μM, $[PO_4]_T = 10$ mM, and Temperature $= 25$ °C. Lines represent model results.
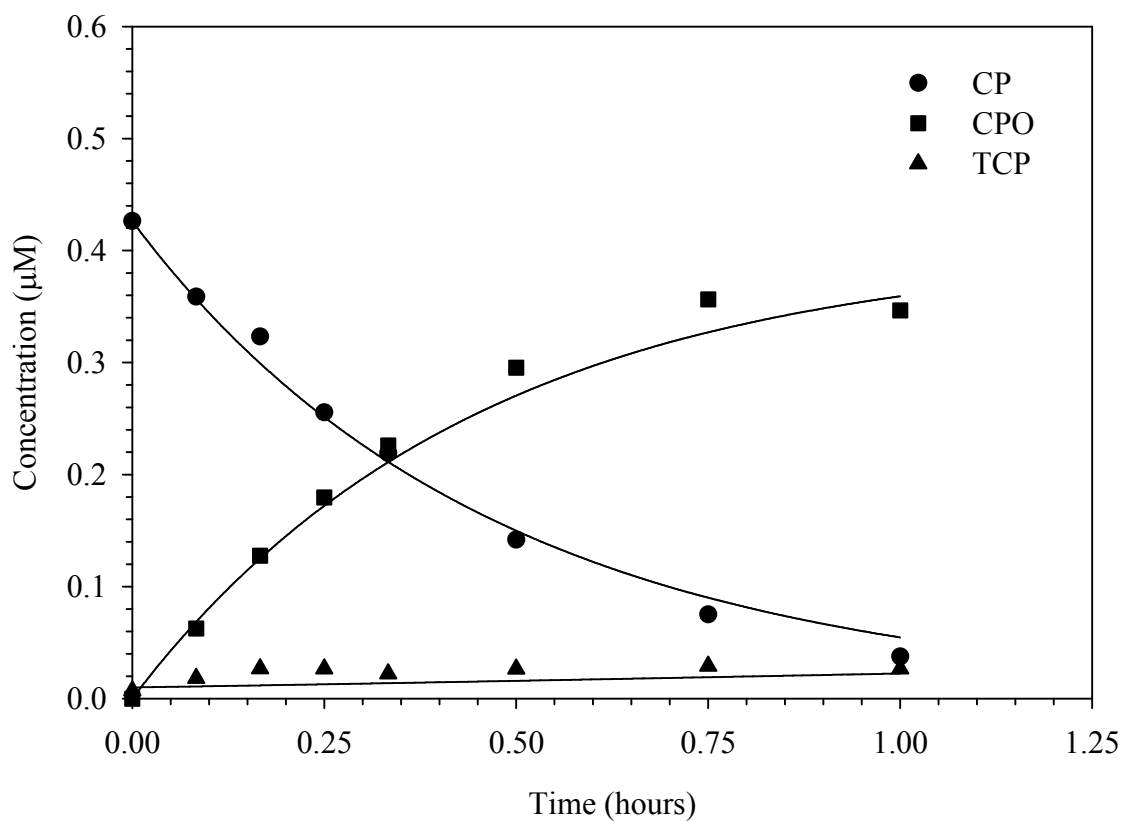
Figure 13   CP degradation in the presence of free chlorine at pH 8.0 in the absence of bromide. $[CP]_o$ = 0.42 μM, $[HOCl]_T$ = 25 μM, $[PO_4]_T$ = 10 mM, and Temperature = 25 ^oC. Lines represent model results.
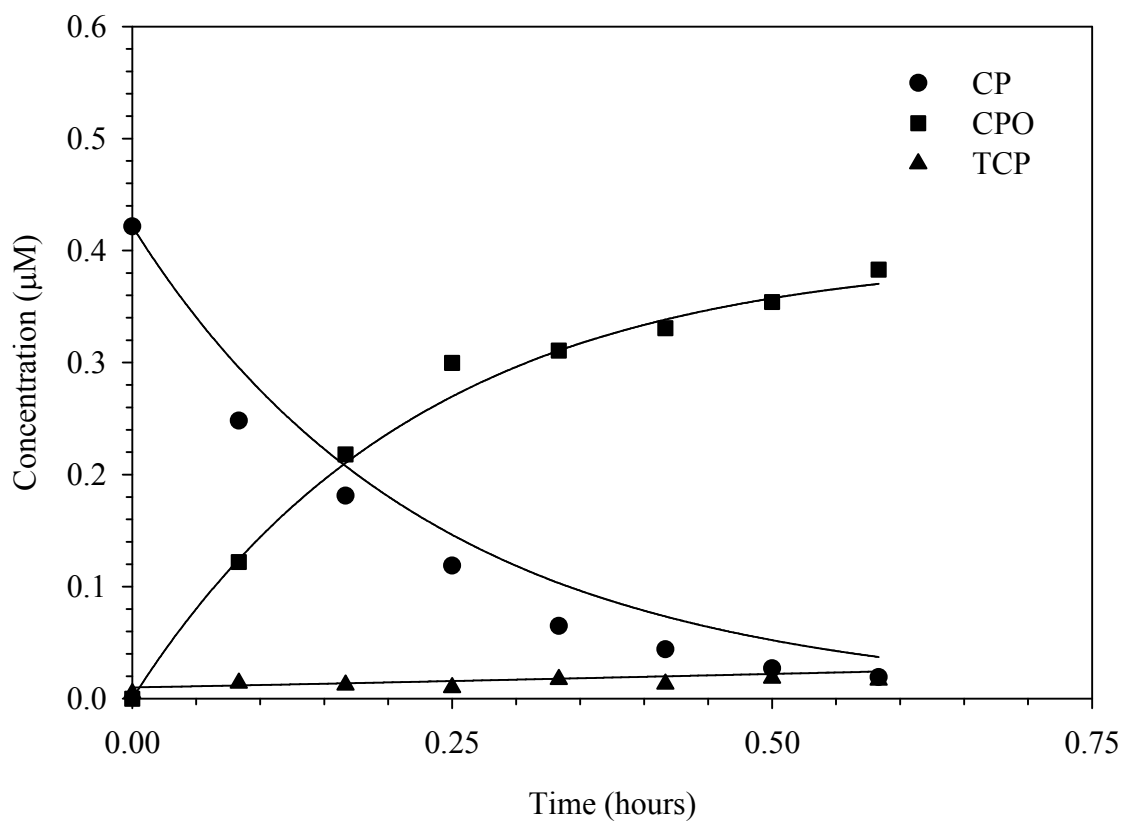
Figure 14   CP degradation in the presence of free chlorine at pH 8.0 in the absence of bromide. $[CP]_o = 0.42 \ \mu M$, $[HOCl]_T = 50 \ \mu M$, $[PO_4]_T = 10$ mM, and Temperature $= 25 \ ^oC$. Lines represent model results.
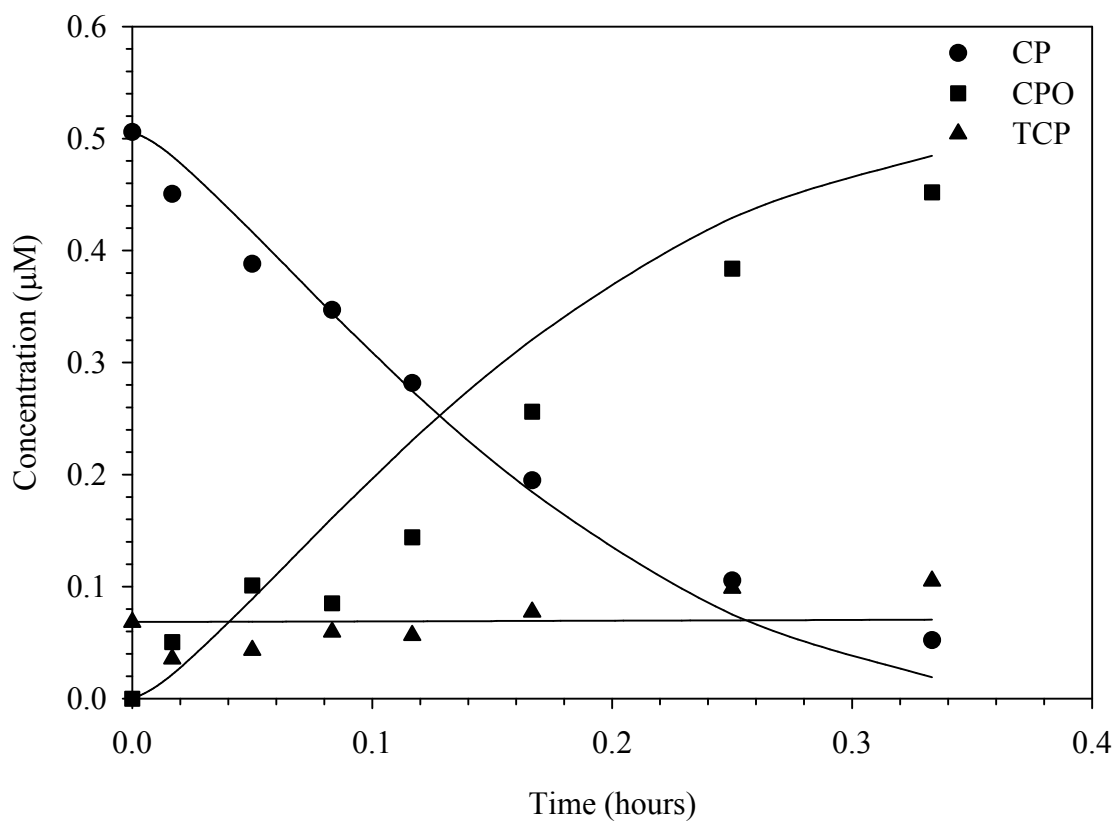
Figure 15   CP degradation in the presence of free chlorine and bromide at pH 8.0. $[CP]_o =$ 0.51 μM, $[HOCl]_T = 10$ μM, $[Br^-] = 1$ μM, $[PO_4]_T = 10$ mM, and Temperature = 25 ^oC. Lines represent model results.
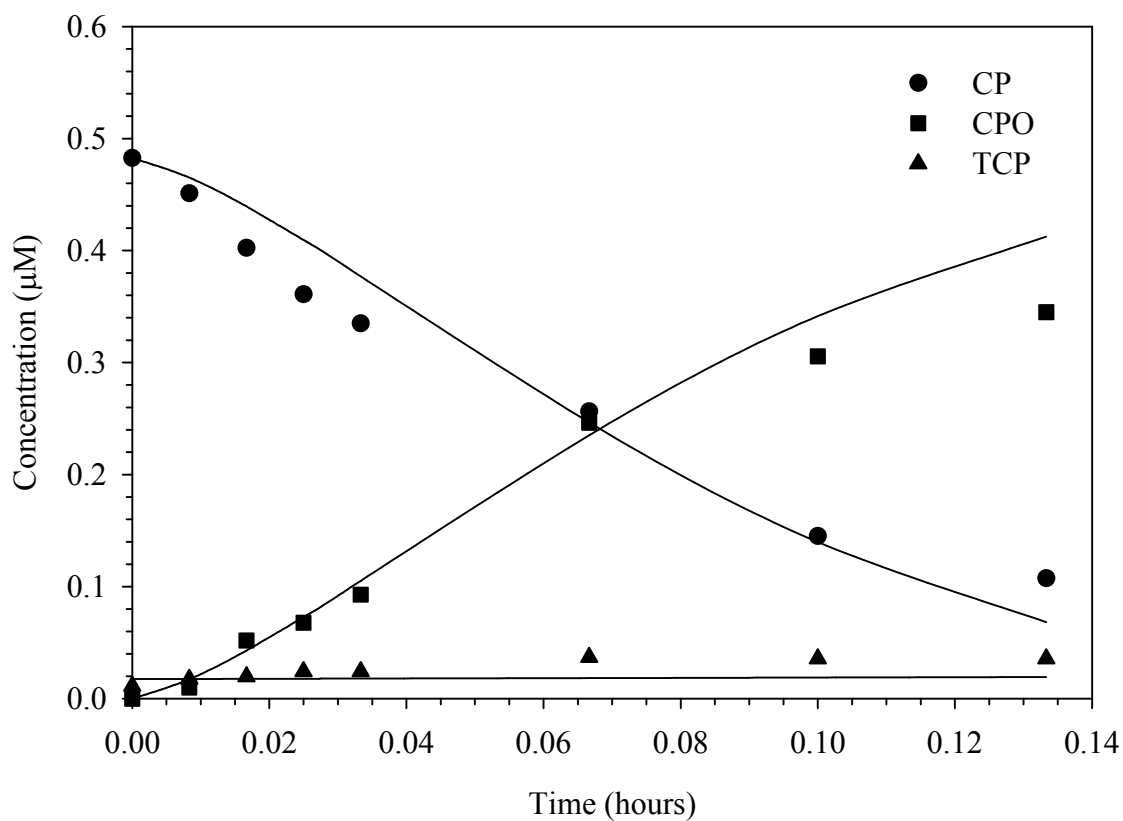
Figure 16   CP degradation in the presence of free chlorine and bromide at pH 8.0. $[CP]_o =$
0.48 μM, $[HOCl]_T = 25$ μM, $[Br^-] = 1$ μM, $[PO_4]_T = 10$ mM, and Temperature = 25
^{o}C. Lines represent model results.
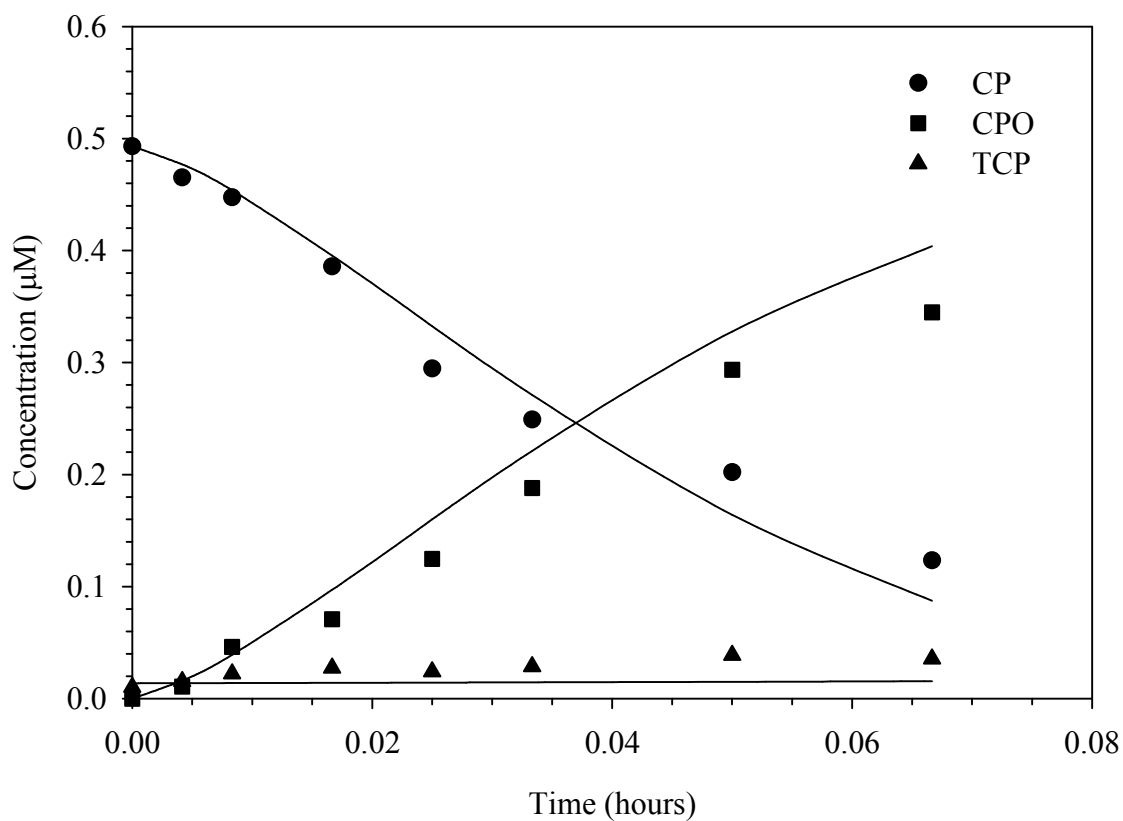
Figure 17   CP degradation in the presence of free chlorine and bromide at pH 8.0. $[CP]_o$ = 0.49 μM, $[HOCl]_T$ = 50 μM, $[Br^-]$ = 1 μM, $[PO_4]_T$ = 10 mM, and Temperature = 25 °C. Lines represent model results.
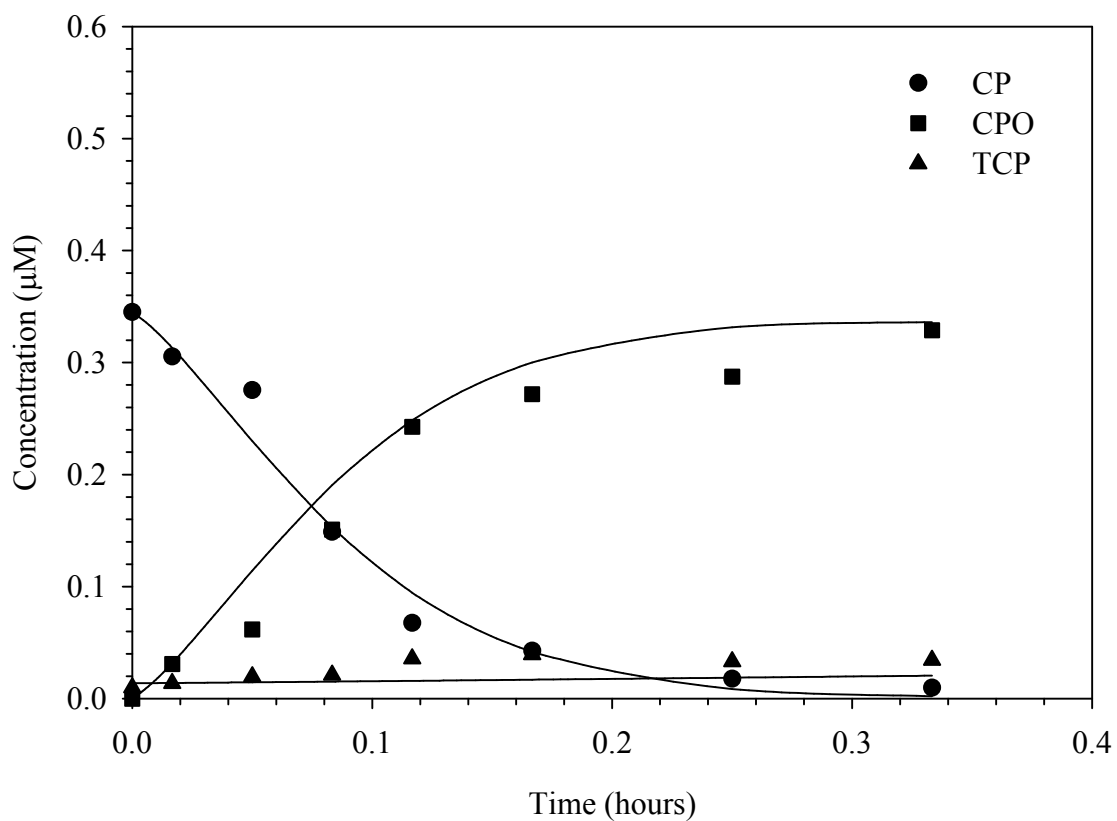
Figure 18   CP degradation in the presence of free chlorine and bromide at pH 8.0. $[CP]_o =$ 0.35 μM, $[HOCl]_T = 50$ μM, $[Br^-] = 1$ μM, $[PO_4]_T = 10$ mM, and Temperature = 25 ^{o}C. Lines represent model results.
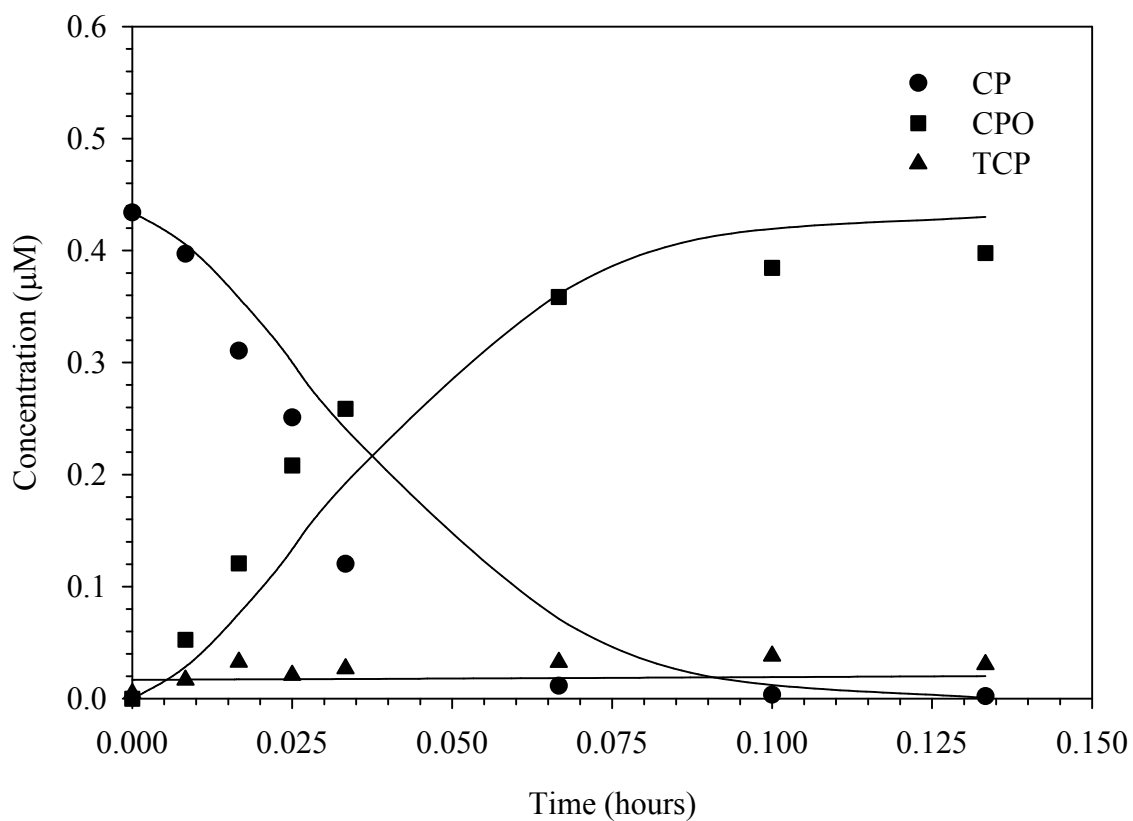
Figure 19   CP degradation in the presence of free chlorine and bromide at pH 8.0. $[CP]_o =$ 0.43 μM, $[HOCl]_T = 50$ μM, $[Br^-] = 5$ μM, $[PO_4]_T = 10$ mM, and Temperature = 25 ^oC. Lines represent model results.
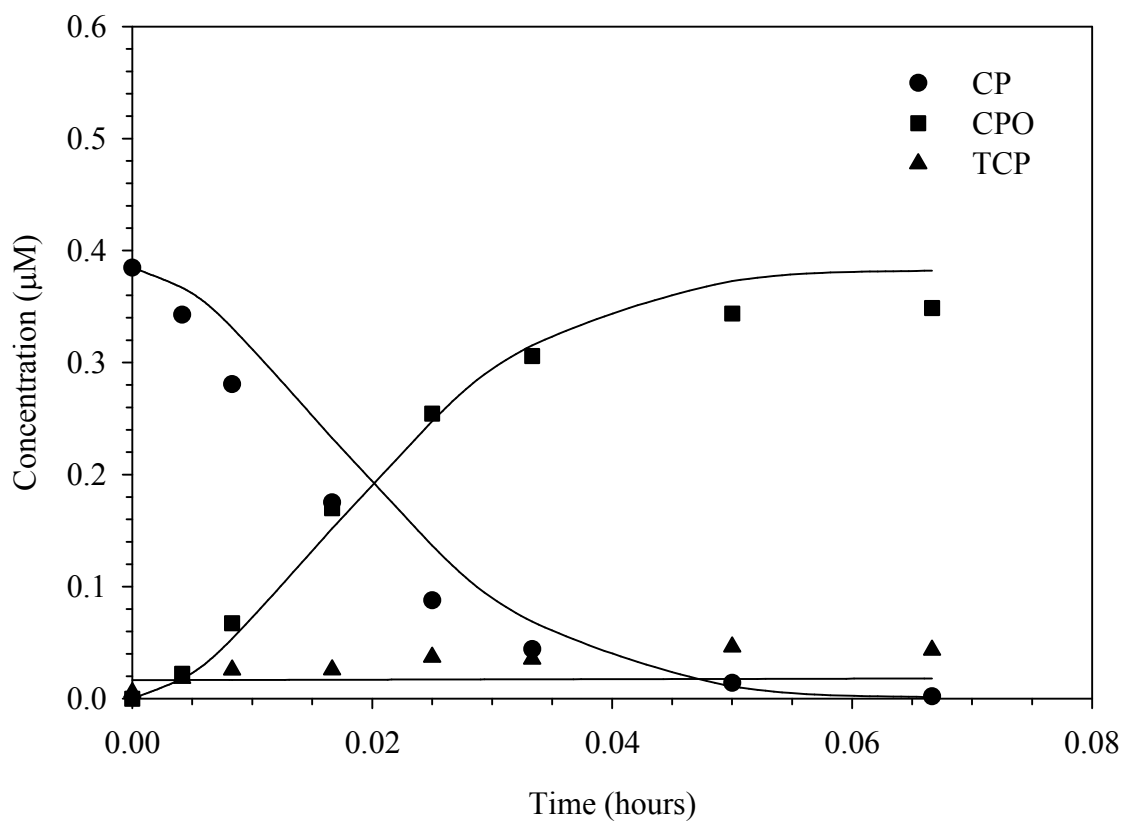
Figure 20   CP degradation in the presence of free chlorine and bromide at pH 8.0. $[CP]_o$ = 0.39 μM, $[HOCl]_T$ = 50 μM, $[Br^-]$ = 10 μM, $[PO_4]_T$ = 10 mM, and Temperature = 25 °C. Lines represent model results.
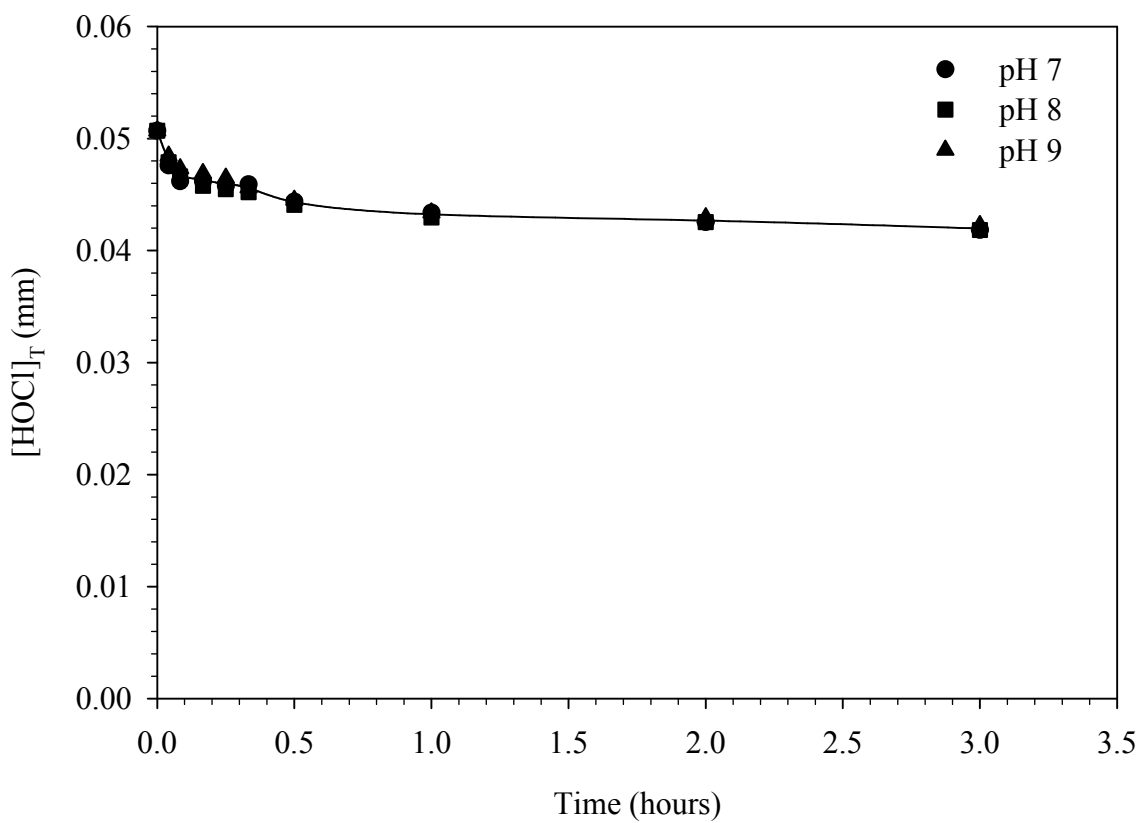
Figure 21   Chlorine demand of ACC water over the pH range of 7-9. $[HOCl]_T = 50~\mu M$, $[Buffer]_T = 10$ mM, $[DOC] = 1.1$ mg-C/L, and Temperature = 25 ^{o}C.
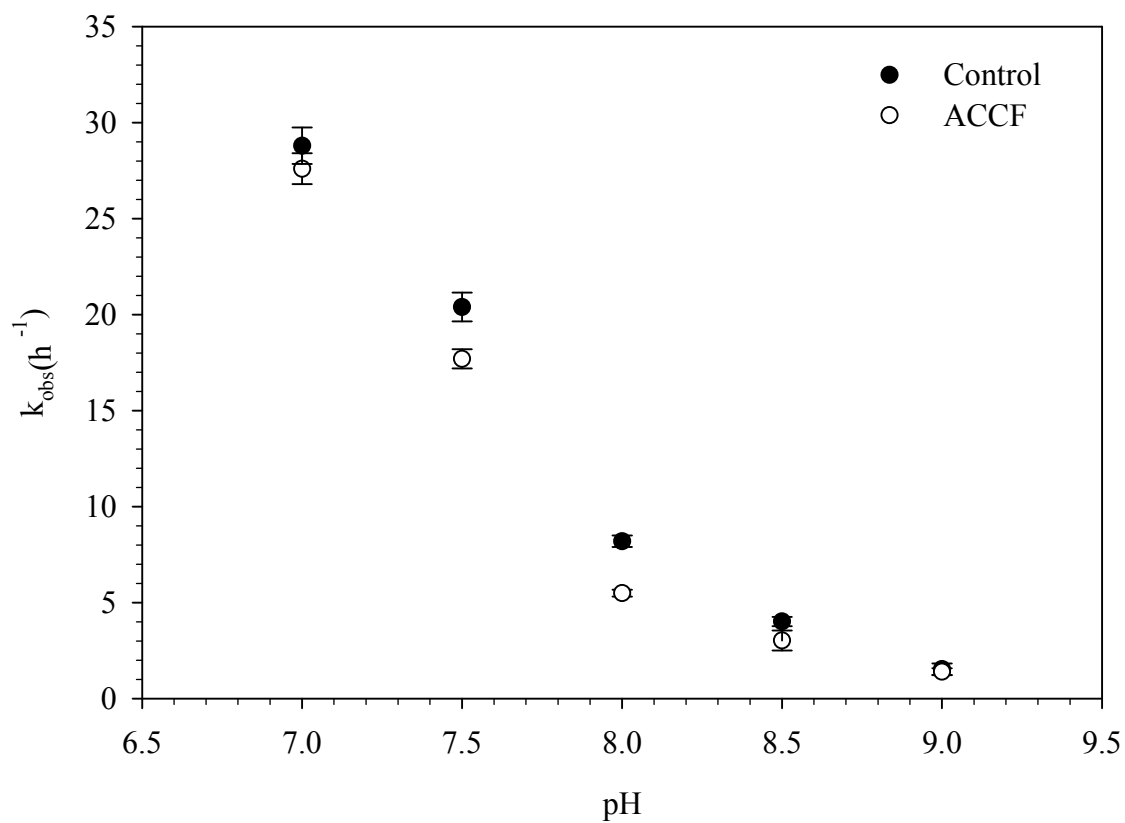
Figure 22   CP degradation in the presence of free chlorine and ACC water over the pH range
of 7-9. $[CP]_o \approx 0.5 \ \mu M$, $[HOCl]_T = 50 \ \mu M$, $[DOC] = 1.1$ mg-C/L, $[Buffer]_T = 10$
mM, and Temperature = 25 ^{o}C. Lines represent model results.
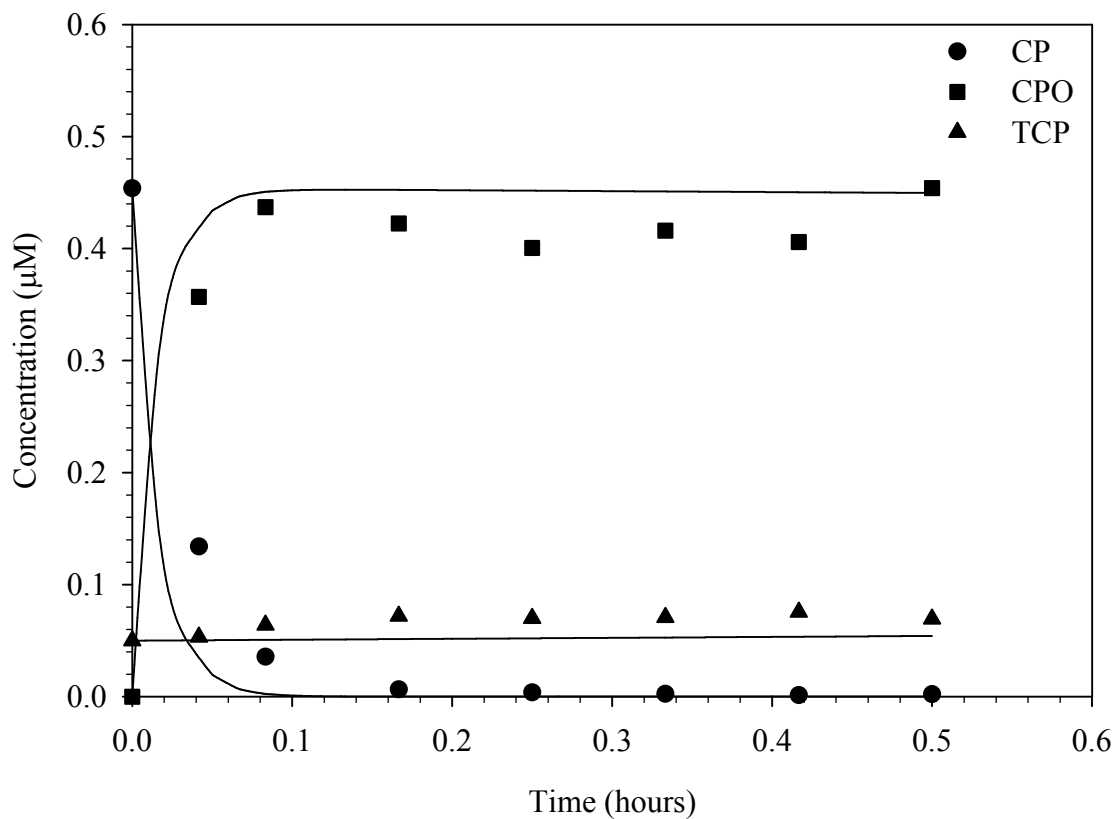
Figure 23   CP degradation in the presence of free chlorine and ACC water at pH 7. $[CP]_o$ = 0.46 μM, $[HOCl]_T$ = 50 μM, $[DOC]$ = 1.1 mg-C/L, $[Buffer]_T$ = 10 mM, and Temperature = 25 ^{o}C. Lines represent model results.
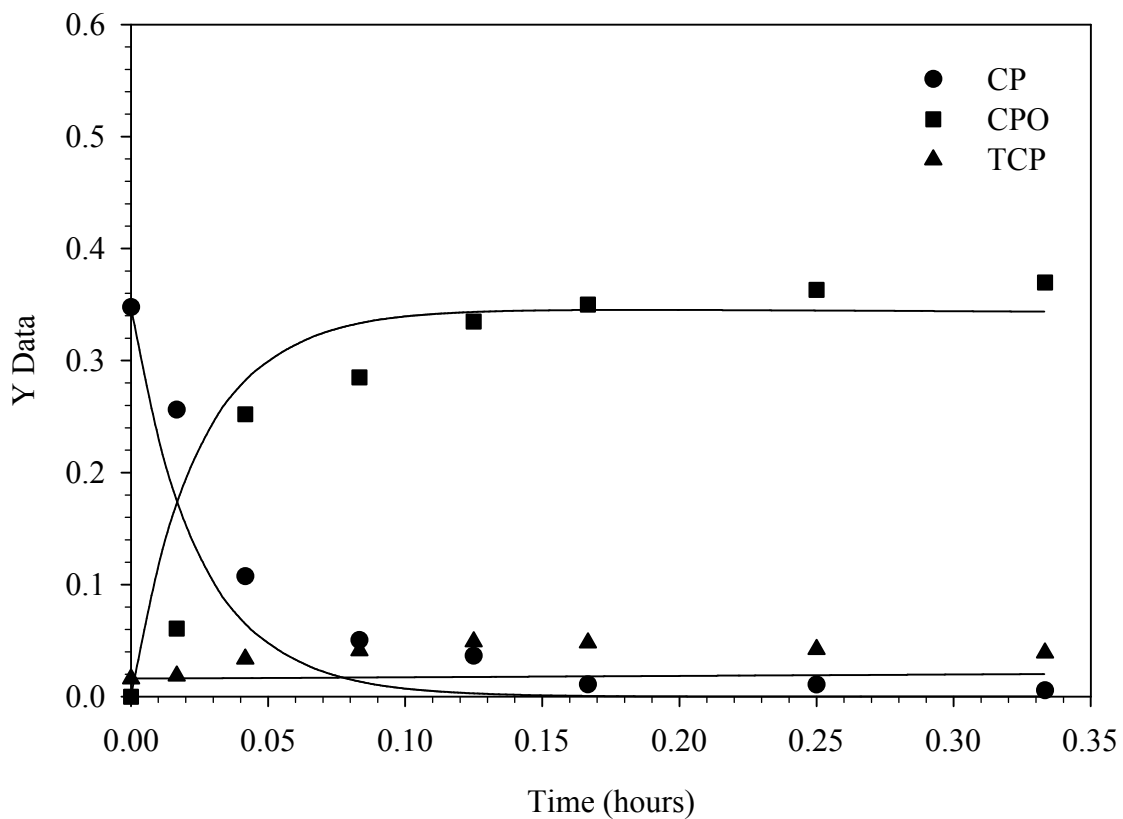
Figure 24   CP degradation in the presence of free chlorine and ACC water at pH 7.5. $[CP]_o$ = 0.35 μM, $[HOCl]_T$ = 50 μM, $[DOC]$ = 1.1 mg-C/L, $[Buffer]_T$ = 10 mM, and Temperature = 25 ^{o}C. Lines represent model results.
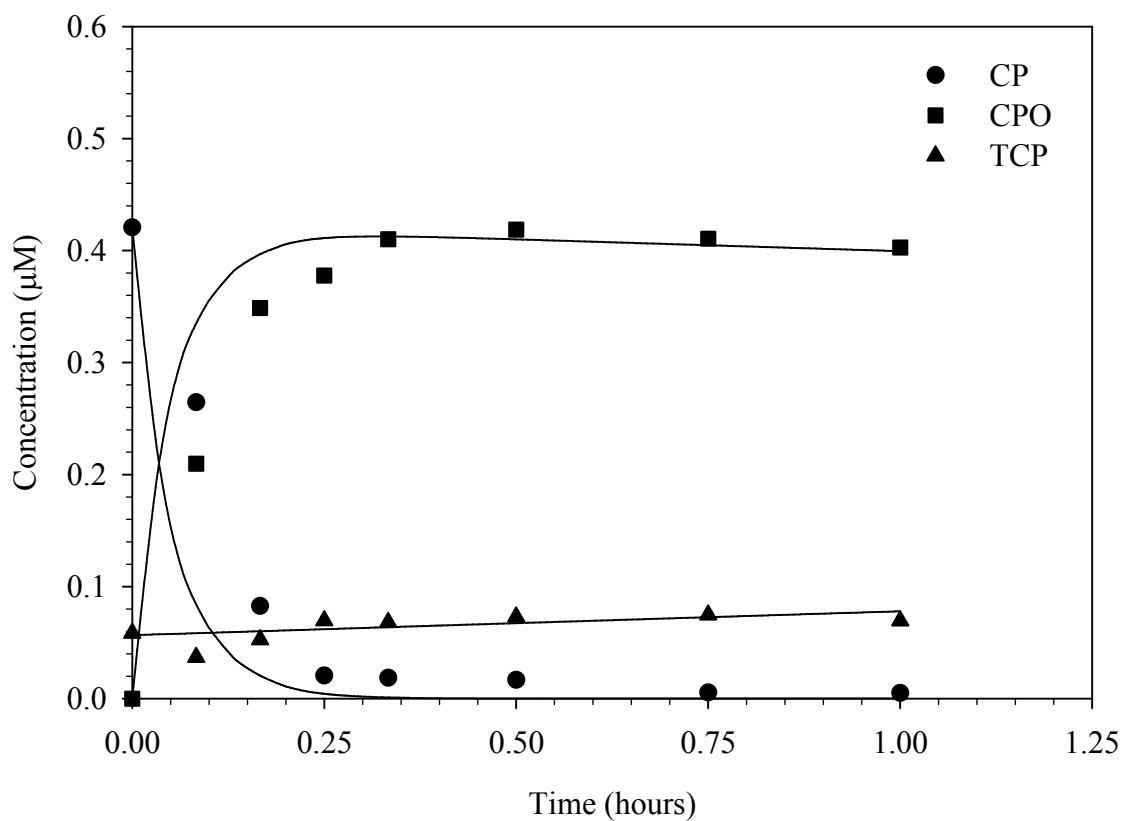
Figure 25   CP degradation in the presence of free chlorine and ACC water at pH 8.0. $[CP]_o$ = 0.42 μM, $[HOCl]_T$ = 50 μM, [DOC] = 1.1 mg-C/L, $[Buffer]_T$ = 10 mM, and Temperature = 25 °C. Lines represent model results.

Figure 26   CP degradation in the presence of free chlorine and ACC water at pH 8.5. $[CP]_o =$ 0.35 µM, $[HOCl]_T = 50$ µM, $[DOC] = 1.1$ mg-C/L, $[Buffer]_T = 10$ mM, and Temperature = 25 °C. Lines represent model results.

Figure 27   CP degradation in the presence of free chlorine and ACC water at pH 9.0. $[CP]_o$ = 0.5 μM, $[HOCl]_T$ = 50 μM, $[DOC]$ = 1.1 mg-C/L, $[Buffer]_T$ = 10 mM, and Temperature = 25 ^{o}C. Lines represent model results.